Supporting Information

Phenphosphine-X (O, S, Se) Locking Multi-resonance Thermally Activated Delayed Fluorescence Materials

Xian-Fang Hong#, Yi Wei#, Hao-Ran Xing#, Yu Wang, Jia-Qi Xi, Chen-Yang Wu, Li Yuan*, Cheng-Hui Li, You-Xuan Zheng*

State Key Laboratory of Coordination Chemistry, Jiangsu Key Laboratory of Advanced Organic Materials, School of Chemistry and Chemical Engineering, Nanjing University, Nanjing, 210023, P. R. China.
E-mail: yxzheng@nju.edu.cn, yl@nju.edu.cn
X.-F. Hong, Y. Wei, and H.-R. Xing contributed this work equally.

Contents

1. General information

The starting reactants and solvents were used as commercial grade without further purification. NMR measurements were conducted on a Bruker AM 400 spectrometer. High-resolution mass spectra were recorded on a MICROTOF-Q III instrument. Thermogravimetric analysis (TGA) measurements were performed on a Pyris 1 DSC under nitrogen at a heating rate of 10 ℃ min^{-1}.

Absorption and photoluminescence spectra were measured on a UV-3100 spectrophotometer and a Hitachi F-4600 photoluminescence spectrophotometer, respectively. The absolute photoluminescence efficiencies (Φ_{PL}) were measured with HORIBA FL3 fluorescence spectrometer. The prompt and decay lifetimes were measured with an Edinburgh Instruments FLS980 spectrometer, with a 365 nm LED and microsecond lamp as excitation sources, respectively. But it is unable to get the percentage of prompt and delayed lifetimes from the data tested by this instrument because the difference between prompt and delayed lifetimes is so large that it is difficult to detect them at the same time in the same window. Fluorescence lifetime testing, using an FPGA based TDC-TCSPC module (MODEL: FF4, Orient KOJI Ltd., Tianjin, CHN)[3], coupled with a 355 nm pulse laser output of 1 kHz, can achieve uninterrupted testing from 100 ps to ms. At the same time, in logarithmic abscissa mode, it is easy to collect the decay curve in the full time domain and use it for photon number statistics.

All the DFT and TD-DFT calculations were carried out using Gaussian 16 software package[1] based on density functional theory (DFT) and time-dependent density functional theory (TD-DFT). The ground and excited state geometry optimizations for all molecules were performed at b3lyp/svp level of theory. On the basis of the optimized structures, TD-DFT calculations were performed at b3lyp/svp level of theory to obtain excited state properties. The electron-hole analysis were generated using the Multiwfn program[2] from the density matrices of DFT calculations. The singlet-triplet energy gap (ΔE_{ST}) was corrected using the spin-component-scaled algebraic-diagrammatic-construction second-order [SCS-ADC(2)] method.

Glass substrates (2.98 × 2.98 × 1.1 cm) pre-coated with a 185 nm thin layer and a sheet resistance of 6 Ω per square of indium tin oxide (ITO) were thoroughly cleaned by ultrasonic of various detergents. OLEDs were fabricated onto the cleaned ITO-coated glass substrates. The organic materials were deposited at a rate of 1 Å s^{-1}, and the Liq and Al films were deposited at rates of 0.2 and 5 Å s^{-1}, respectively, under high vacuum ($\leq 1 \times 10^{-4}$ Pa). The EL spectra were measured with a calibrated Hitachi F-4600 fluorescence spectrophotometer. Based on the uncorrected EL fluorescence spectra, the Commission Internationale de l'Eclairage (CIE) coordinates were calculated using the test program of Spectrascan PR650 spectrophotometer. The electroluminescence performances were measured by the Keithley 2400 and Keithley 2000 electroluminescence measurement system. The EQEs of EL devices were calculated based on the photo energy measured by the photodiode, the EL spectrum and the current pass through the device.

2. Experiment section

2.1 Synthesis routes and procedures for NBNPO, NBNPS and NBNPSe.

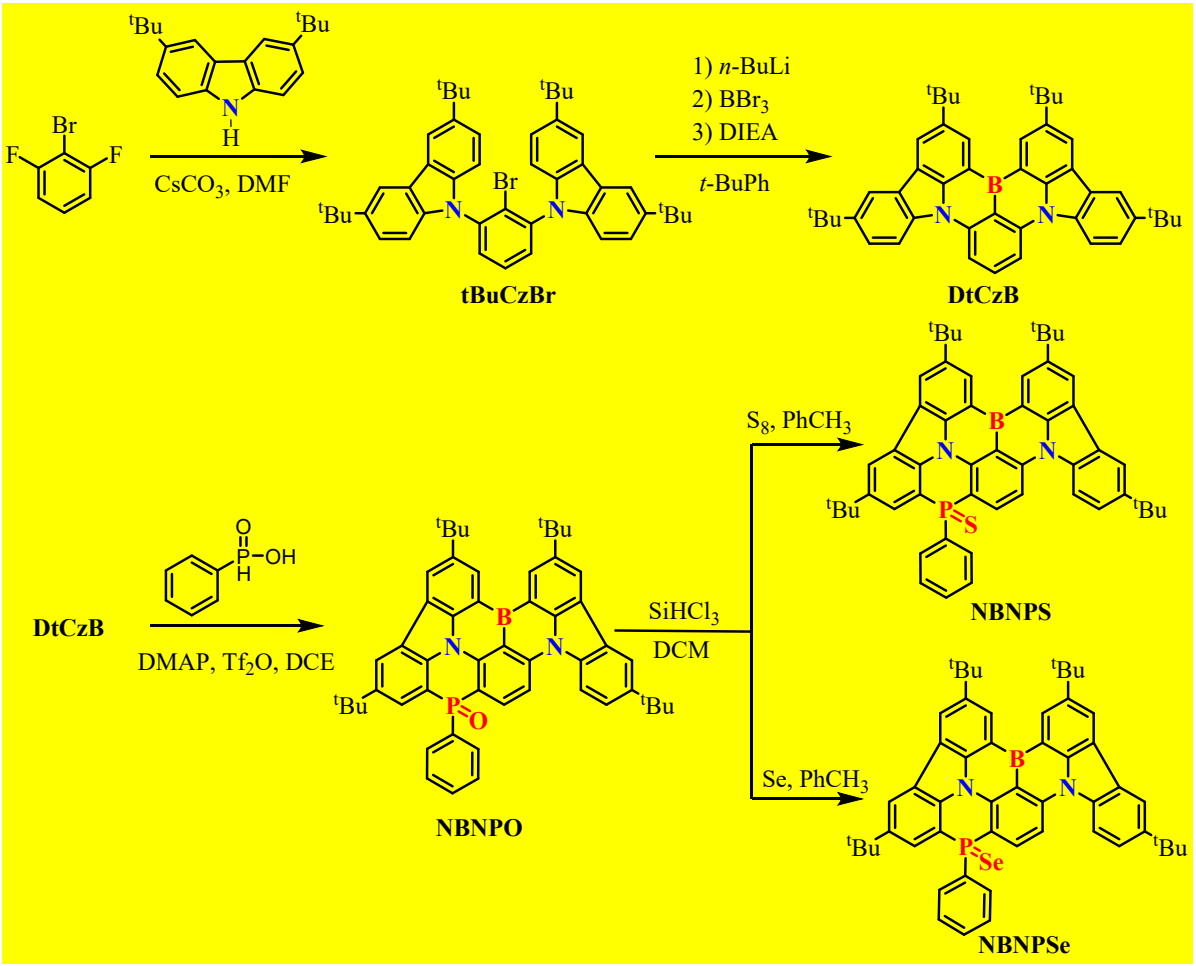

Scheme S1. Synthetic procedure of the precursors and compounds.

Synthesis of ^{t}BuCzBr: 60 mL solution of anhydrous DMF (*N*,*N*-dimethylformamide) which contains 3,6-di-*tert*-butyl 9*H*-carbazole (9.75 g, 35.2 mmol) was added dropwise into a mixture of *t*-BuOK (4.90 g, 43.8 mmol) and 50 mL anhydrous DMF in a period of 15 min. After the system was stirring for 2 h at room temperature, 20 mL anhydrous DMF solution containing 2-bromo-1,3-difluorobenzene (3.10 g, 16.0 mmol) was injected dropwise within 15 min. The solution was stirred at 140 °C for 24 h and then cooled down. The resulted solution was poured into ice water (2000 g). The white powder solid was filtered out and dried in vacuum, further purified by column chromatography with using a mixture eluent of dichloromethane/ petroleum ether (v:v, 1:3), resulting in a white solid (9.10 g, yield: 80%). ^{1}H NMR (400 MHz, Chloroform-*d*) δ 8.20 (s, 4H), 7.72-7.64 (m, 3H), 7.56-7.51 (m, 4H), 7.16 (d, *J* = 8.4 Hz, 4H), 1.51 (s, 36H). ^{13}C NMR (101 MHz, Chloroform-*d*) δ 143.11, 139.67, 139.29, 130.89, 129.28, 125.85, 123.83, 123.40, 116.49, 109.42, 34.82, 32.09.

Synthesis of DtCzB: A solution of *tert*-butyllithium in *n*-hexane (19.4 mL, 1.3 M, 25.2 mmol) was added slowly to a solution of compound 1 (9.00 g, 12.6 mmol) in *tert*-butylbenzene (100 mL) at –30 ºC under a nitrogen atmosphere. After stirring at 60 ºC for 2 h, *n*-hexane was removed in vacuum. After addition of boron tribromide (2.4 mL, 25.2 mmol) at –30 ºC, the reaction mixture was stirred at room

temperature for 1 h. *N*,*N*-Diisopropylethylamine (3.5 mL, 25.2 mmol) was added at 0 ºC and then the reaction mixture was allowed to room temperature. After stirring at 130 ºC for 5 h, the reaction mixture was cooled to room temperature. 5 mL methanol was added to the reaction mixture to quench residual BBr_3. The aqueous layer was separated and extracted with 200 mL dichloromethane. The combined organic layer was condensed in vacuum and purified by column chromatography with a mixture eluent of dichloromethane/petroleum ether (v:v, 1:20), resulting in a bright yellow solid (2.10 g, yield: 26%). ^{1}H NMR (400 MHz, Chloroform-*d*) δ/ppm: 9.09 (d, *J* = 1.7 Hz, 2H), 8.45 (d, *J* = 1.8 Hz, 2H), 8.29 (d, *J* = 8.8 Hz, 2H), 8.26 (d, *J* = 2.0 Hz, 2H), 8.16 (d, *J* = 8.0 Hz, 2H), 7.83 (t, *J* = 8.2 Hz, 1H), 7.63 (dd, *J* = 8.8, 2.0 Hz, 2H), 1.71 (s, 18H), 1.57 (s, 18H). ^{13}C NMR (101 MHz, Chloroform-*d*) δ/ppm: 145.18, 144.51, 144.19, 141.52, 138.35, 132.90, 129.78, 127.04, 124.31, 123.60, 121.57, 120.60, 117.22, 114.12, 107.90, 35.19, 34.80, 32.24, 31.87.

Synthesis of NBNPO: In a Schlenk tube, phenylphosphinic acid (1.11 g, 7.8 mmol), DtBuCz (1.24 g, 1.9 mmol), and 4-dimethylaminopyridine (2.27 g, 18.6 mmol) were placed in 1,2 dichloroethane (18 mL) under N_2. Trifluoromethanesulfonic anhydride (3.1 mL, 18.6 mmol) was then added at room temperature. The reaction mixture was heated at 90 ºC in an oil bath for 24 hours. Finally, the reaction mixture was allowed to cool to room temperature, and poured into 30 mL of water. The organic layer was extracted with dichloromethane, dried over anhydrous Na_2SO_4. The solvent was removed under vacuum. After purification by silica gel column chromatography (eluent: dichloromethane/ethyl acetate, v/v = 4:1), a yellow powdery solid was obtained (1.2 g, yield: 85%). ^{1}HNMR (400 MHz, Chloroform-*d*) δ/ppm: 9.21-9.20 (m, 2H), 8.58 (s, 1H), 8.50 (d, *J* = 7.8 Hz, 2H), 8.42-8.32 (m, 3H), 8.26 (s, 1H), 8.05-8.01 (m, 1H), 7.81-7.76 (m, 2H), 7.64 (d, *J* = 8.24 Hz, 1H), 7.47 (s, 3H), 1.71-1.70 (m, 18H), 1.53 (s, 9H), 1.50 (s, 9H). ^{13}C NMR (101 MHz, Chloroform-*d*) δ 147.56, 147.46, 146.49, 146.16, 145.65, 141.43, 140.89, 140.32, 138.23, 137.27, 135.29, 131.75, 131.64, 131.48, 130.45, 129.76, 129.05, 128.55, 128.42, 128.24, 127.50, 125.30, 125.16, 124.84, 124.50, 123.35, 122.59, 122.34, 121.44, 119.88, 117.48, 114.63, 109.46, 109.35, 35.53, 35.47, 35.26, 34.87, 32.24, 32.15, 31.92, 31.78. ESI-MS (M): $C_{52}H_{52}BN_2OP$ m/z: 762.7848 [M]+ [H] (calcd: 763.3969).

Synthesis of NBNPS: Under N_2 atmosphere, NBNPO (0.76 g, 1 mmol), trichlorosilane (1.0 mL, 10 mmol) and 5 mL of dry dichloromethane were added in a 100 mL flask, The mixture was stirred for 12 h at room temperature. Finally, the solvent was removed under vacuum. The product was obtained as a yellow powder solid NBNP with a yield of 100%.

Under N_2 atmosphere, NBNP (0.75 g, 1 mmol), sulfur (0.32 g, 10 mmol) and dry toluene (4 mL) were added in a 100 mL Schlenk tube. The reaction mixture was heated at 120 ˚C for 12 h. Finally, the reaction mixture was allowed to cool to room temperature, and poured into 30 mL of water. The organic layer was extracted with dichloromethane, dried over anhydrous Na_2SO_4. The solvent was removed under vacuum. The product was obtained as a yellow powder solid (0.56 g, yield: 73%), which was purified by silica gel column chromatography (dichloromethane/petroleum ether, v:v, 1:1). ^{1}H NMR (400 MHz, Chloroform-*d*) δ/ppm: 9.18-9.16 (m, 2H), 8.55-8.40 (m, 5H), 8.32 (d, *J* = 8.4 Hz, 1H), 8.25 (d, *J* = 4.0

Hz, 1H), 8.06-8.02 (m, 1H), 7.83-7.77 (m, 2H), 7.64-7.62 (m, 1H), 7.38-7.35 (m, 3H), 1.70 (d, J = 2.8 Hz, 18H), 1.52 (s, 9H), 1.50 (s, 9H). ^{13}C NMR (101 MHz, Chloroform-*d*) δ 148.20, 148.10, 146.42, 146.34, 146.12, 145.61, 141.47, 140.31, 139.65, 138.30, 138.20, 137.56, 137.45, 136.07, 131.17, 131.05, 130.96, 130.43, 129.71, 128.50, 128.37, 127.43, 125.60, 125.53, 124.85, 124.48, 123.28, 122.58, 121.76, 121.45, 117.46, 114.56, 113.47, 112.58, 110.12, 110.00, 108.11, 107.22, 35.57, 35.45, 35.24, 34.86, 32.22, 32.13, 31.90, 31.77. ESI-MS (M): $C_{52}H_{52}BN_2SP$ m/z: 778.8458 [M+ H] (calcd: 780.9432).

Synthesis of NBNPSe: NBNPSe was synthesis with the similar procedures as NBNPS, but replacing sulfur with selenium (0.79 g, 10 mmol) with a yield of 61% (0.50 g). ^{1}H NMR (400 MHz, Chloroform-*d*) 9.18-9.16 (m, 2H), 8.54-8.50 (m, 2H), 8.44 (d, J = 8.8 Hz, 1H), 8.37 (s, 1H), 8.32 (d, J = 8.8 Hz, 1H), 8.24 (s, 1H), 8.04 (d, J = 14.8 Hz, 1H), 7.86-7.81 (m, 2H), 7.63 (d, J = 8.8 Hz, 1H), 7.36 (d, J = 2.4 Hz, 3H), 1.69 (d, J = 2.0 Hz, 18H), 1.52 (s, 9H), 1.50 (s, 9H). ^{13}C NMR (101 MHz, Chloroform-*d*) δ 147.23, 147.12, 145.42, 145.16, 144.61, 140.42, 139.18, 138.07, 137.26, 137.15, 135.56, 130.66, 130.54, 130.00, 129.40, 128.67, 127.48, 127.35, 126.40, 125.36, 125.28, 123.83, 123.73, 123.46, 122.23, 121.54, 120.77, 120.43, 116.44, 113.54, 111.17, 110.36, 109.20, 109.08, 105.65, 104.85, 34.56, 34.42, 34.21, 33.83, 31.19, 31.09, 30.84, 30.73. ESI-MS (M): $C_{52}H_{52}BN_2SeP$ m/z: 825.7568 [M+ H] (calcd: 826.4370).

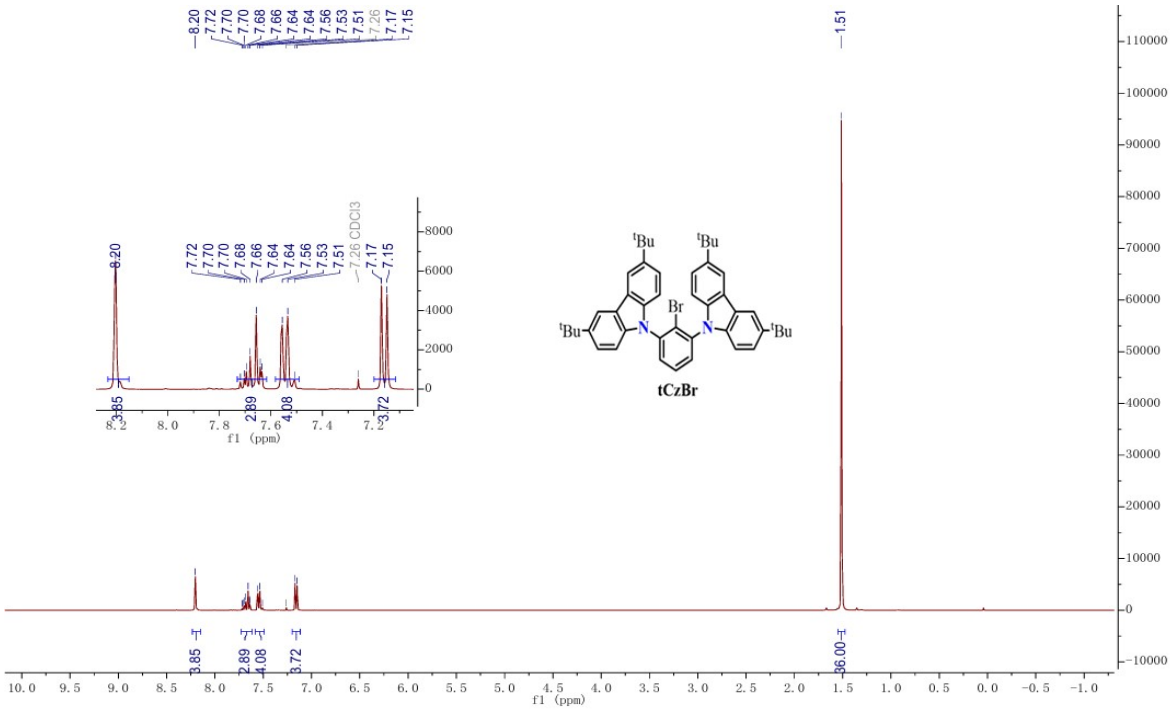

Fig. S1 ^{1}H NMR spectrum of tBuCzBr in chloroform-*d*.

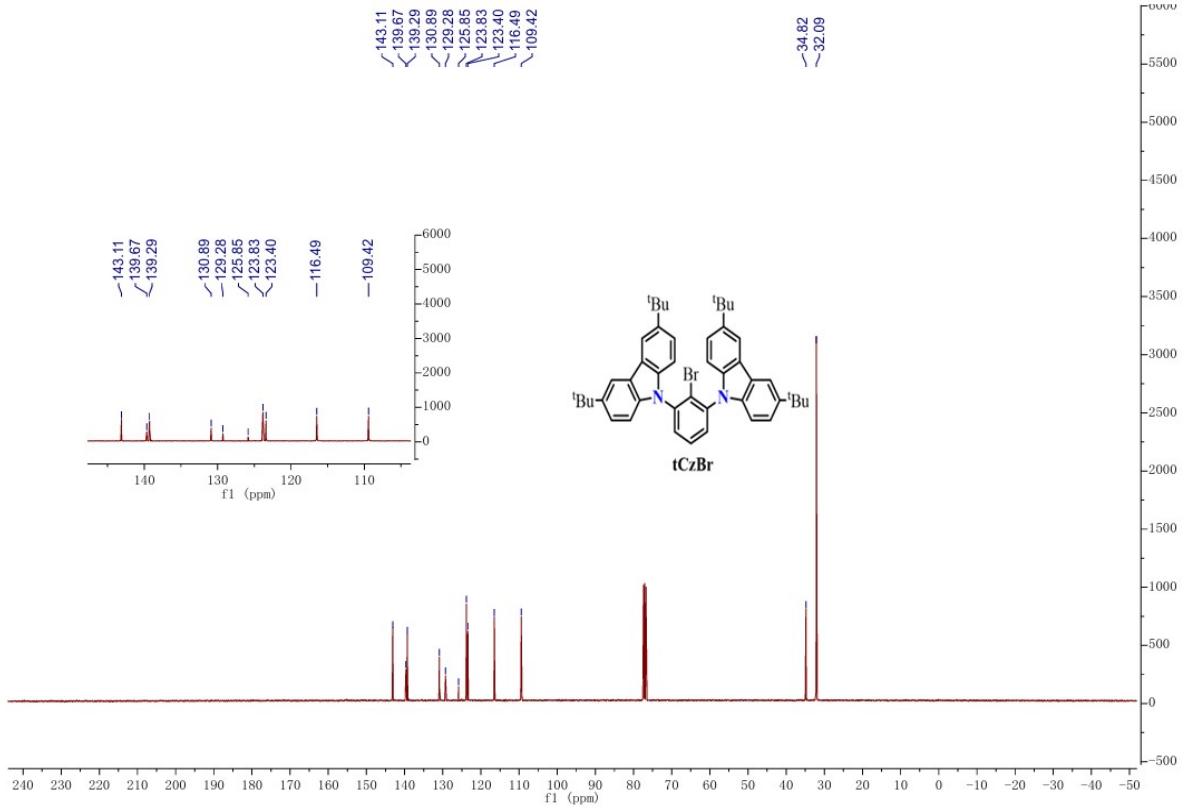

Fig. S2 ^{13}C NMR spectrum of tBuCzBr in chloroform-*d*.

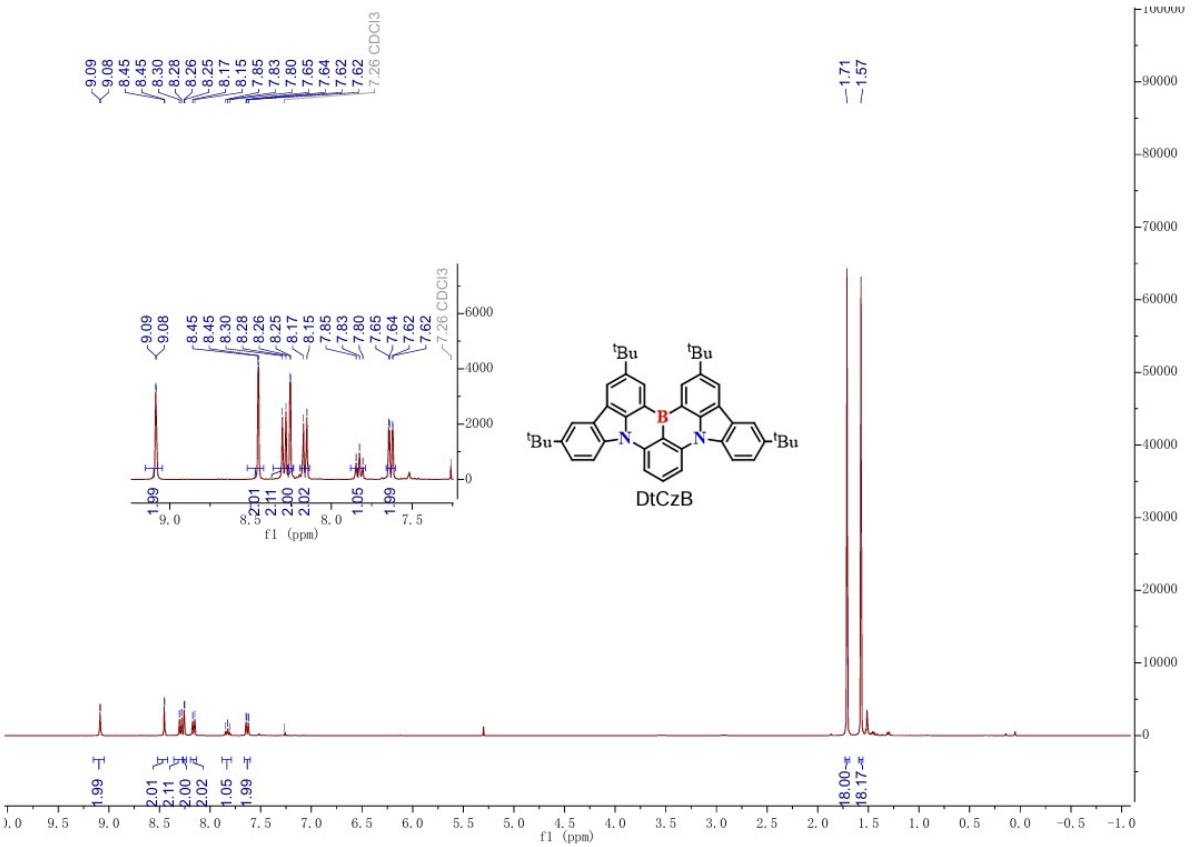

Fig. S3 ^{1}H NMR spectrum of DtCzB in chloroform-*d*.

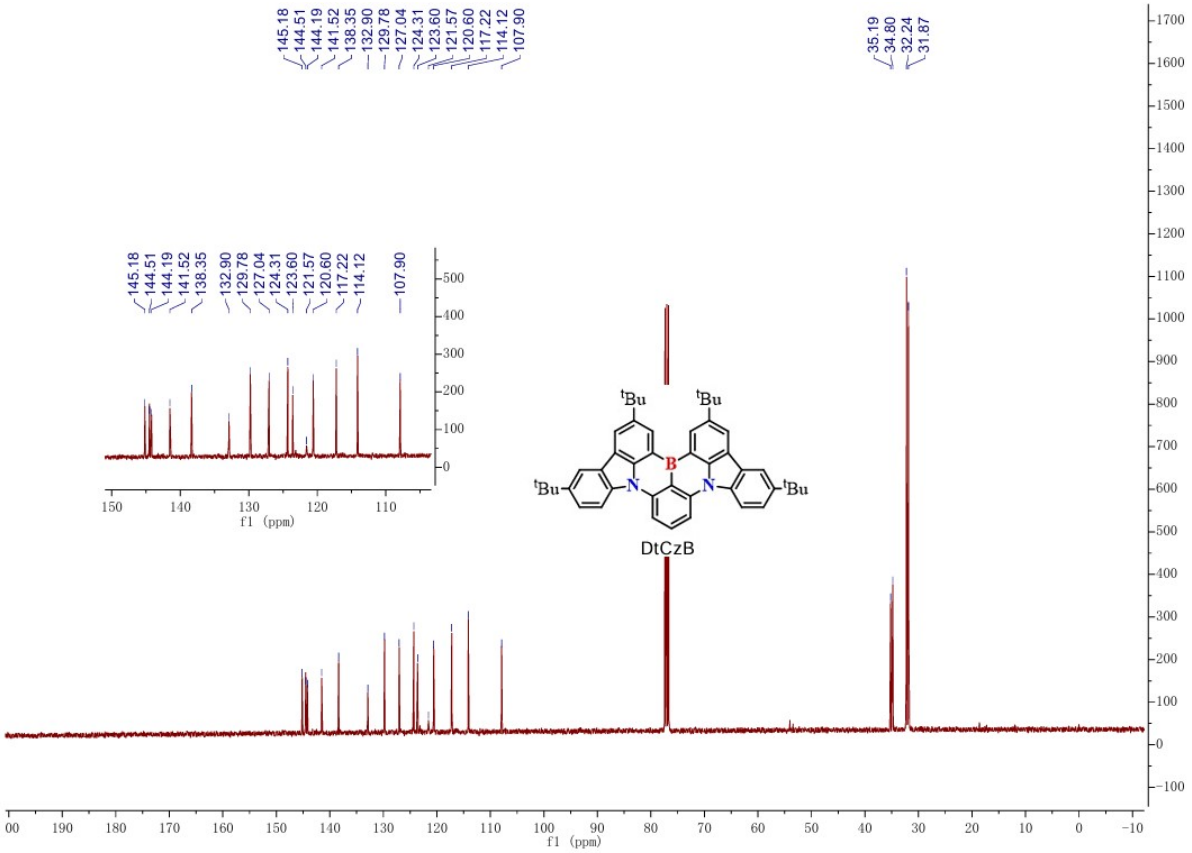

Fig. S4 ^{13}C NMR spectrum of DtCzB in chloroform-*d*.

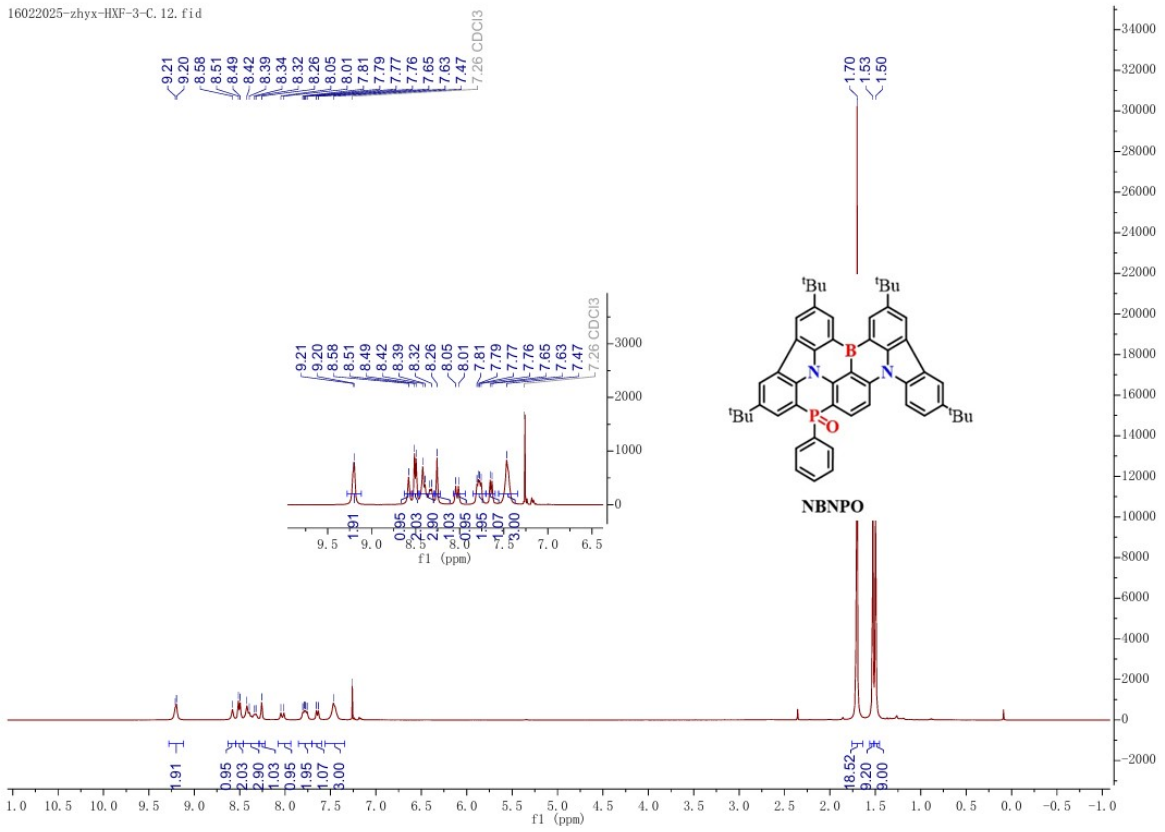

Fig. S5 ^{1}H NMR spectrum of NBNPO in chloroform-*d*.

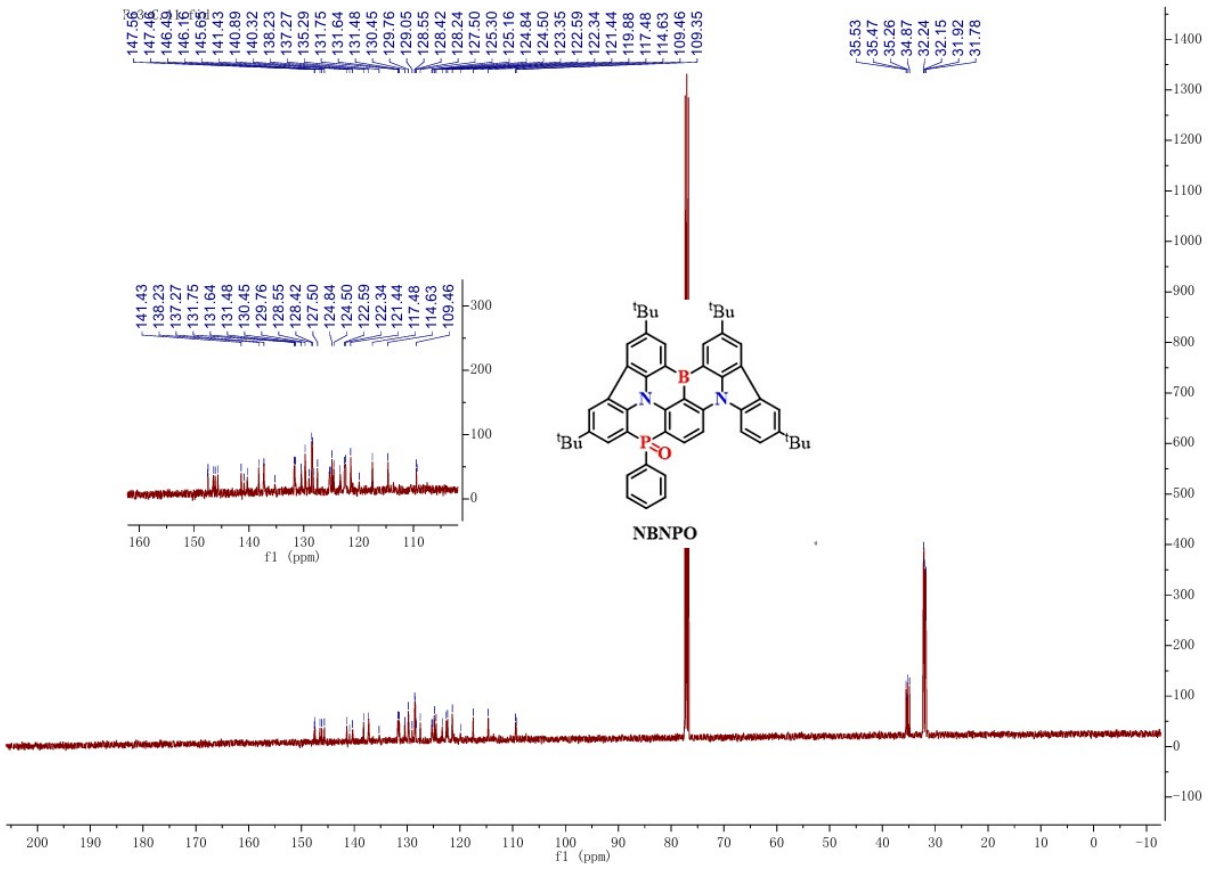

Fig. S6 ^{13}C NMR spectrum of NBNPO in chloroform-*d*.

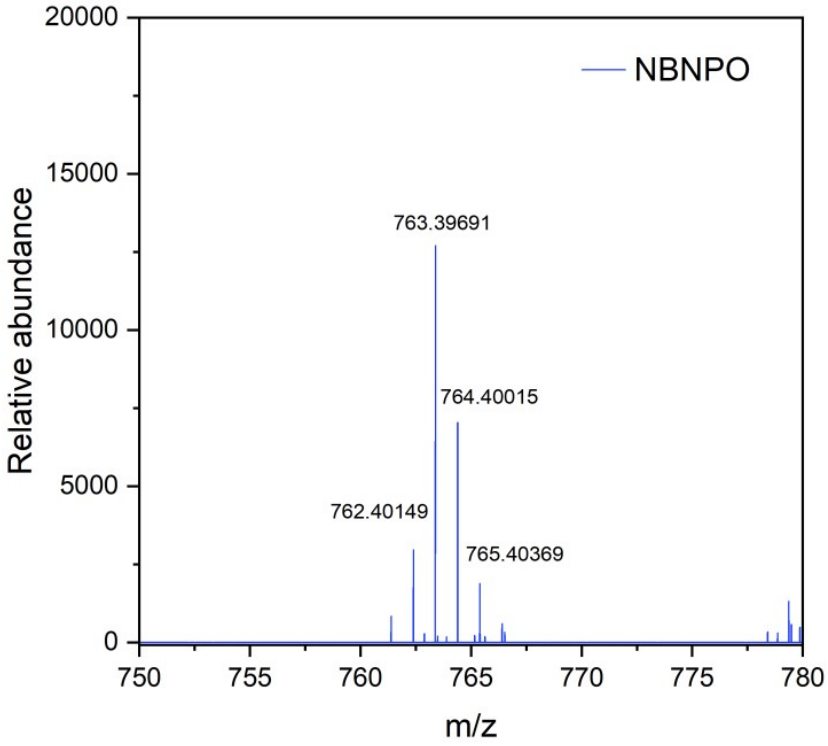

Fig. S7 HRMS spectrum of NBNPO.

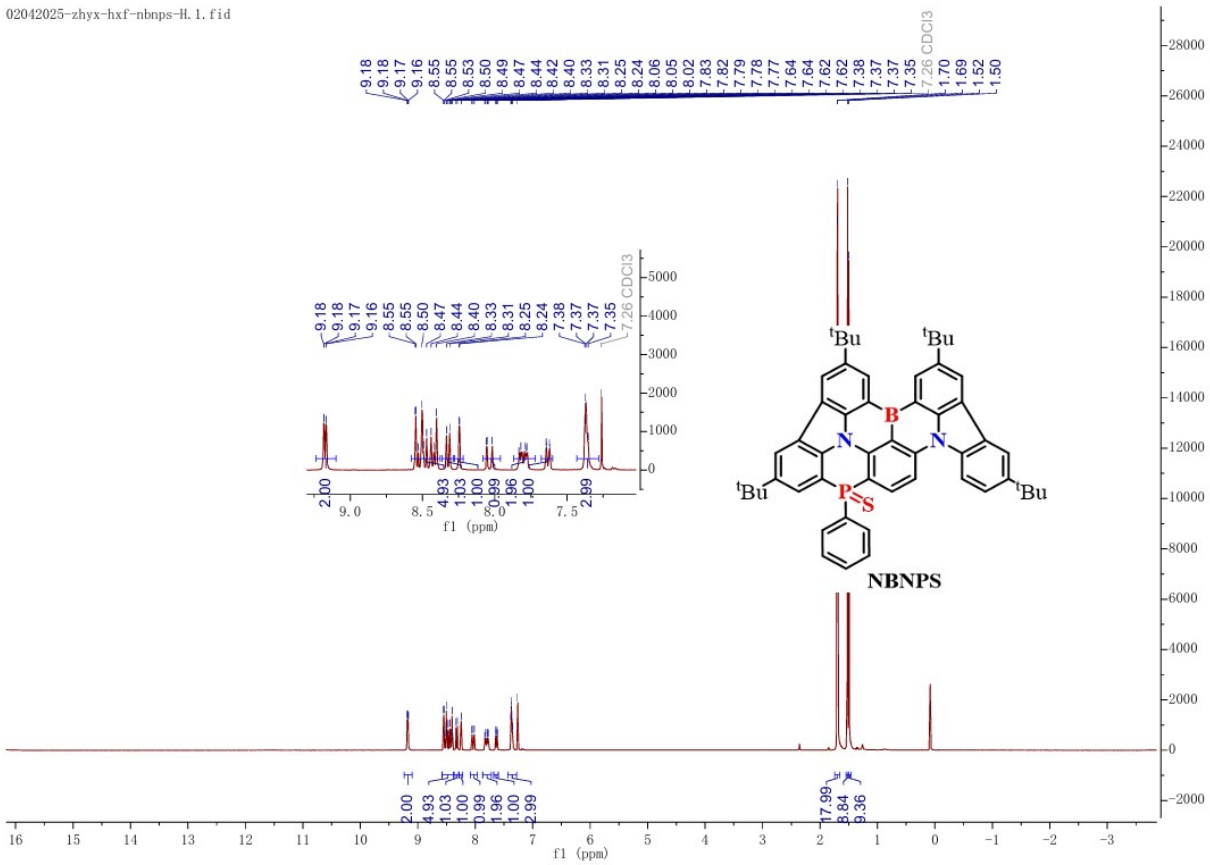

Fig. S8 ^{1}H NMR spectrum of NBNPS in chloroform-*d*.

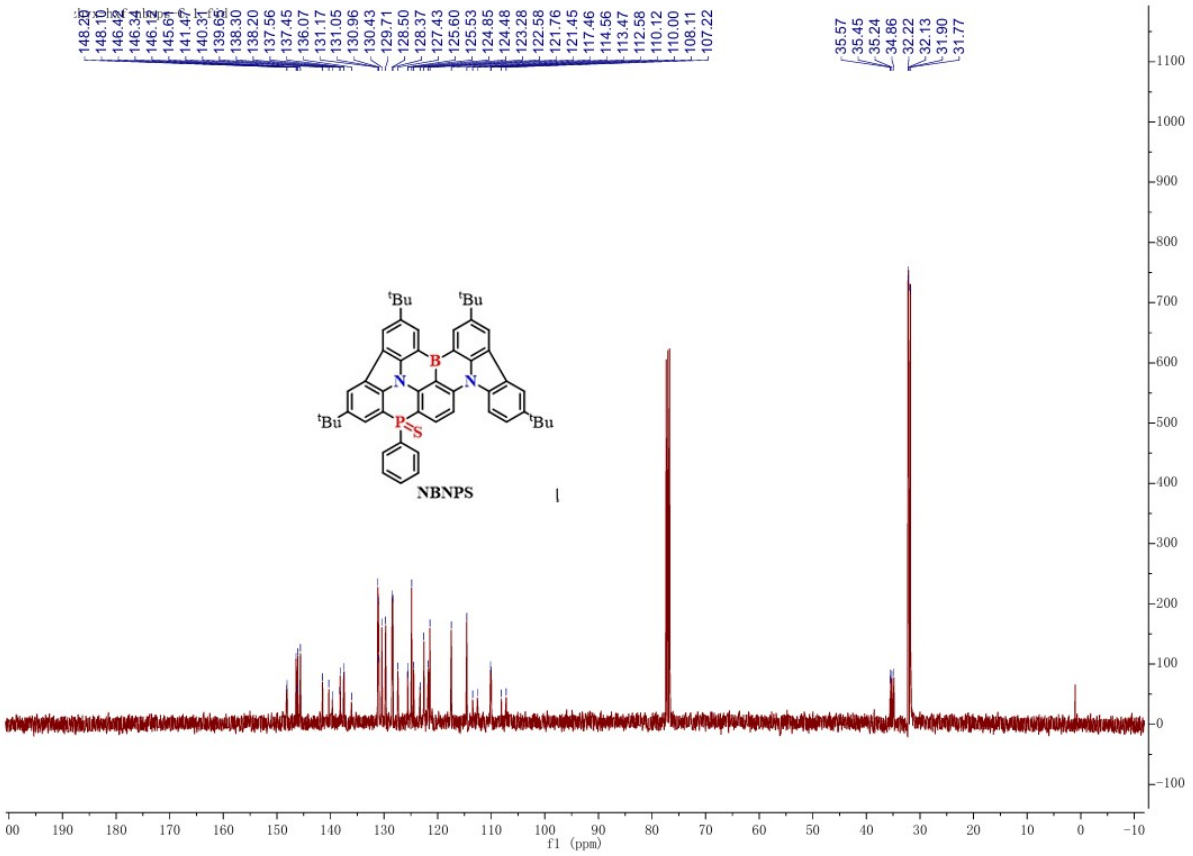

Fig. S9 ^{13}C NMR spectrum of NBNPS in chloroform-*d*.

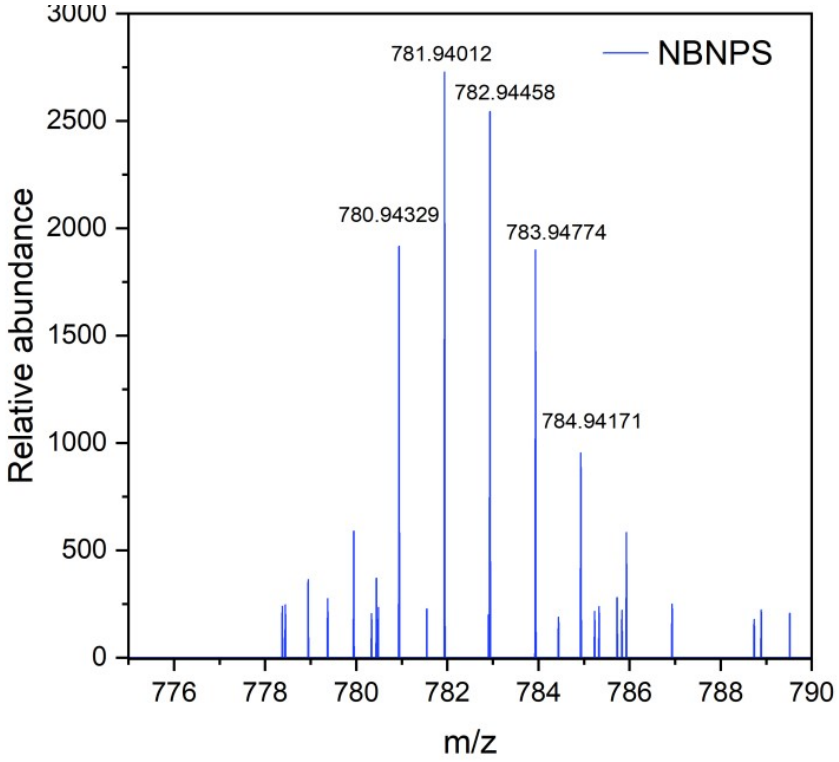

Fig. S10 HRMS spectrum of NBNPS.

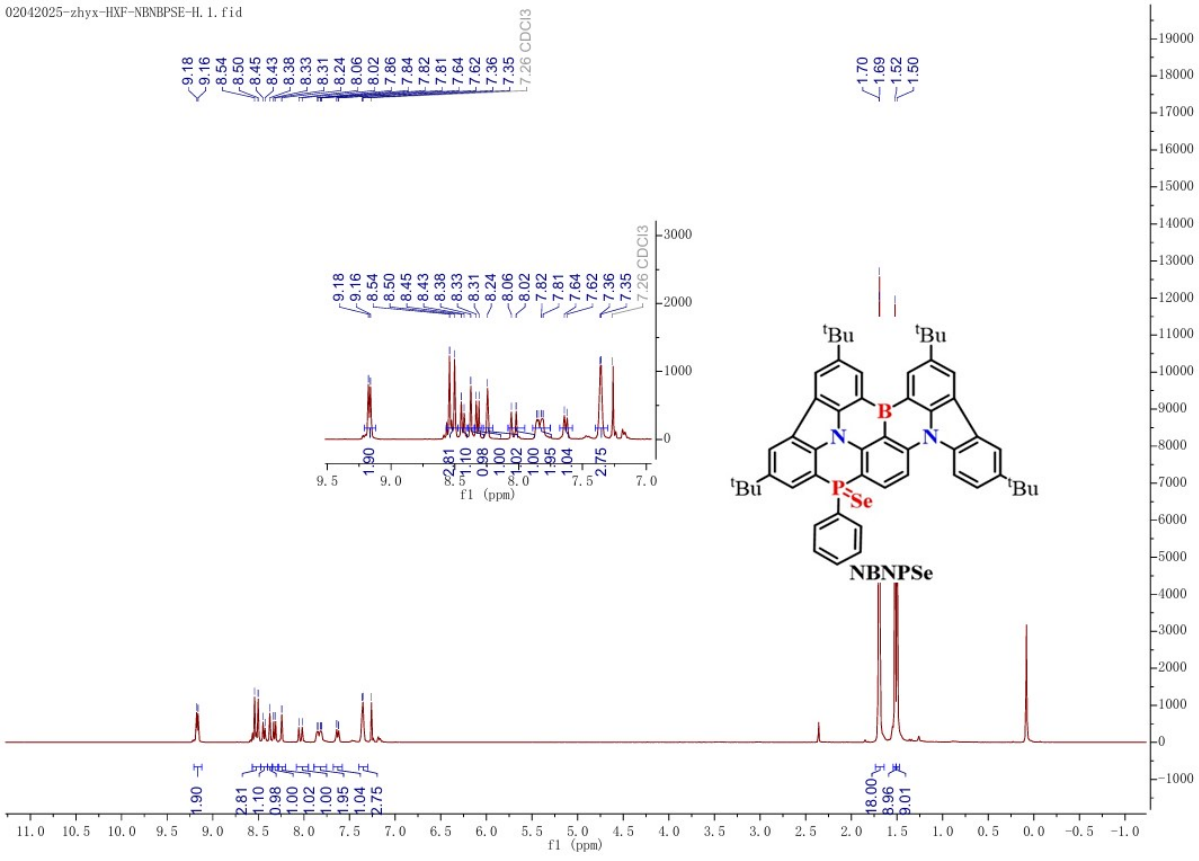

Fig. S11 ^{1}H NMR spectrum of NBNPSe in chloroform-*d*.

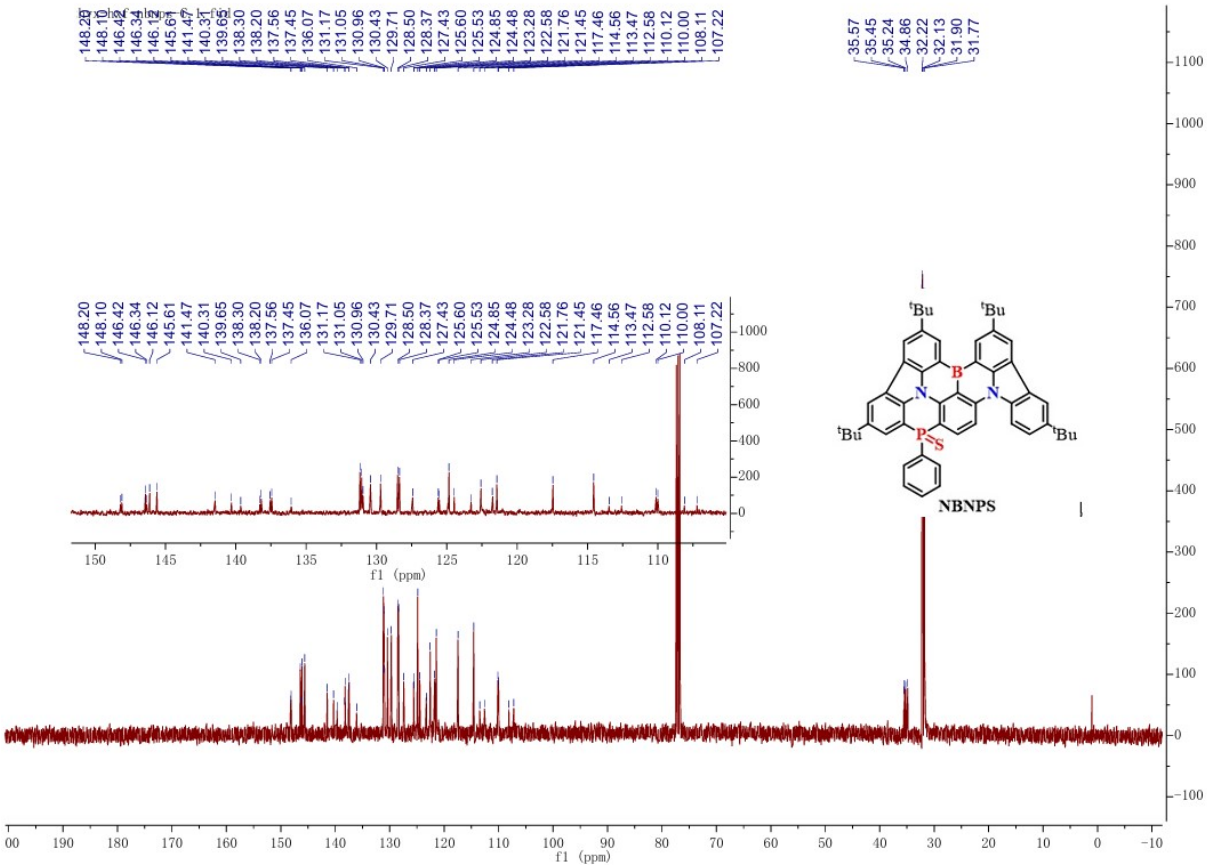

Fig. S12 ^{13}C NMR spectrum of NBNPSe in chloroform-*d*.

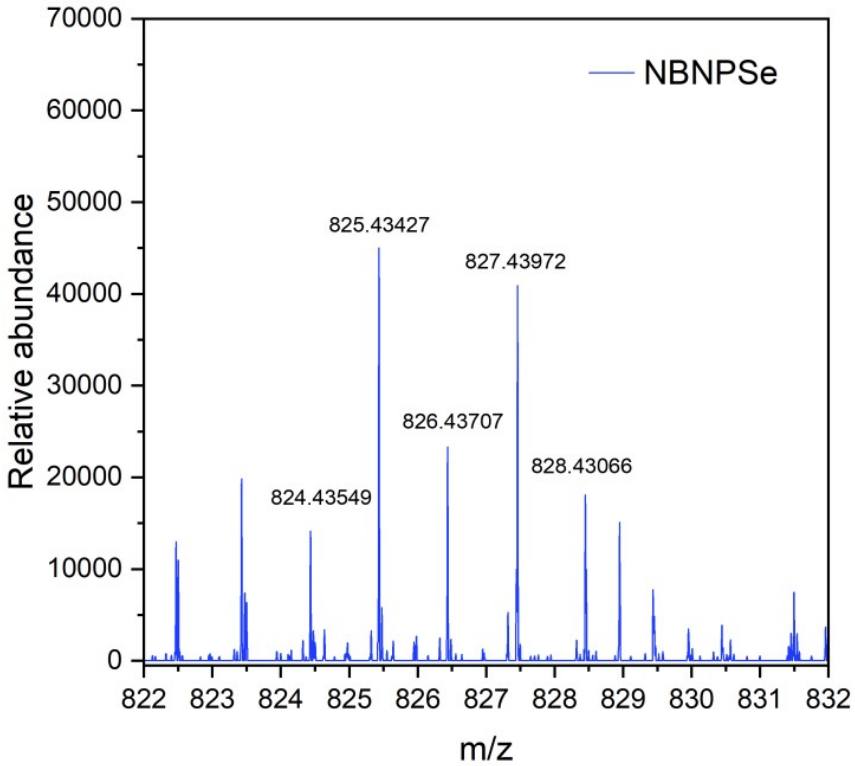

Fig. S13 HRMS spectrum of NBNPSe.

3. Thermal stability

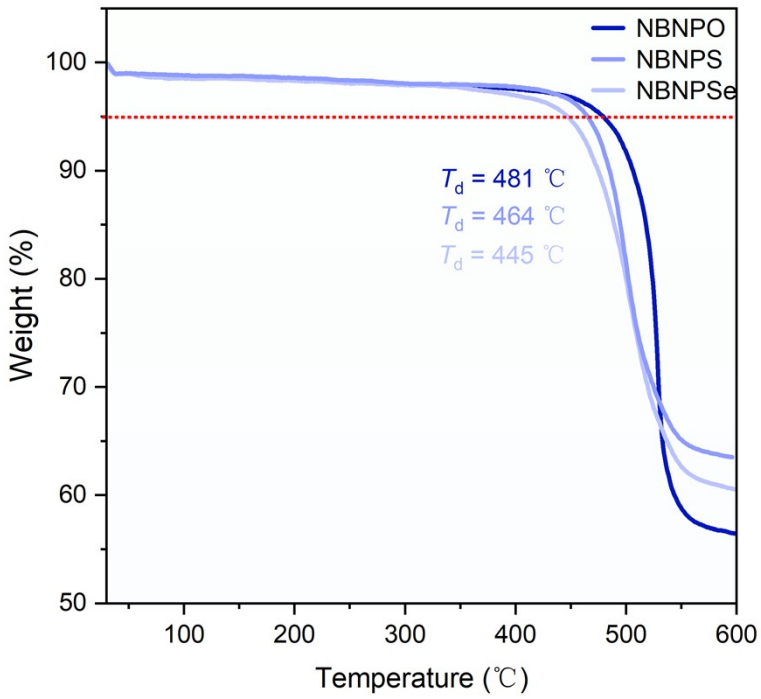

Fig. S14 The TGA curves of NBNPO (T_d = 481 °C),NBNPS (T_d = 464 °C) and NBNPSe (T_d = 445 °C).

4. Electrochemical measurements

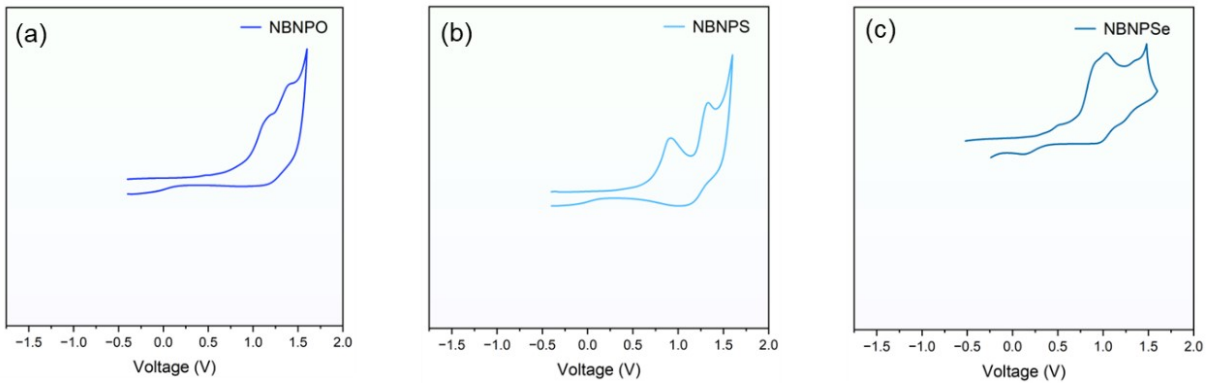

Fig. S15 Cyclic voltammogram curves of NBNPO, NBNPS and NBNPSe in CH_3CN.

Table S1. Cyclic voltammogram curve of NBNPO, NBNPS and NBNPSe in CH_3CN.

Compound	$E_{ox,onset}$	$E_{ox,onset}$ (Fc)	E_g	$E_{HOMO/LUMO}$
NBNPO	1.14	0.53	2.73	-5.41/-2.68
NBNPS	0.92	0.53	2.70	-5.19/-2.49
NBNPSe	0.91	0.53	2.69	-5.18/-2.49

5. X-ray crystallographic data

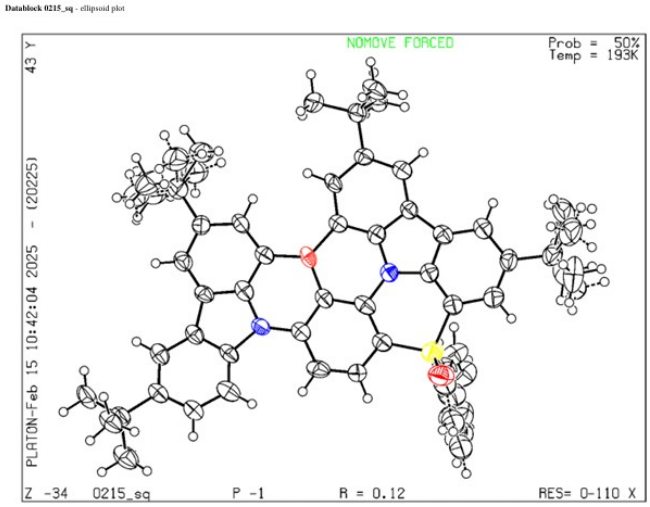

Fig. S16 Single-crystal structure of NBNPO.

Table S2. X-Ray Crystallographic Data and Structure Refinement for NBNPO.

Compound	NBNPO
CCDC No.	2452671
Formula	$C_{52}H_{52}BN_2OP$
Formula weight	762.78
T (K)	193.00
Wavelength (Å)	0.71073
Crystal system	Triclinic
Space group	$P\bar{1}$
a (Å)	10.7415(19)
b (Å)	13.639(3)
c (Å)	16.481(3)
α (deg)	92.727(5)
β (deg)	97.742(5)
γ (deg)	99.273(5)
V (Å^3)	2355.3(8)
Z	2
ρ_{calcd} (mg m^{-3})	1.205
μ (Mo Kα) (mm^{-1})	0.102
F (000)	912.0
Radiation	MoKα (λ = 0.71073)
2Θ range for data collection/°	3.792 to 50.052
Reflns collected	15755
Index ranges	-12 ≤ h ≤ 12 -11 ≤ k ≤ 16 -19 ≤ l ≤ 19
Independent reflections	8230 [R_{int} = 0.1586, R_{sigma} = 0.1723]
Data/restraints/params	8230/234/620
GOF on F^2	1.035
R_1[a], wR_2[b][$I > 2\sigma(I)$]	0.1191, 0.2822
R_1[a], wR_2[b](all data)	0.1995,0.3333
Largest diff. peak/hole / e Å^{-3}	0.37/-0.47

R_1[a] = $\sum||F_o|-|F_c||/\sum F_o|$. wR_2[b] = $[\sum w(F_o^2-F_c^2)^2/\sum w(F_o^2)]^{1/2}$

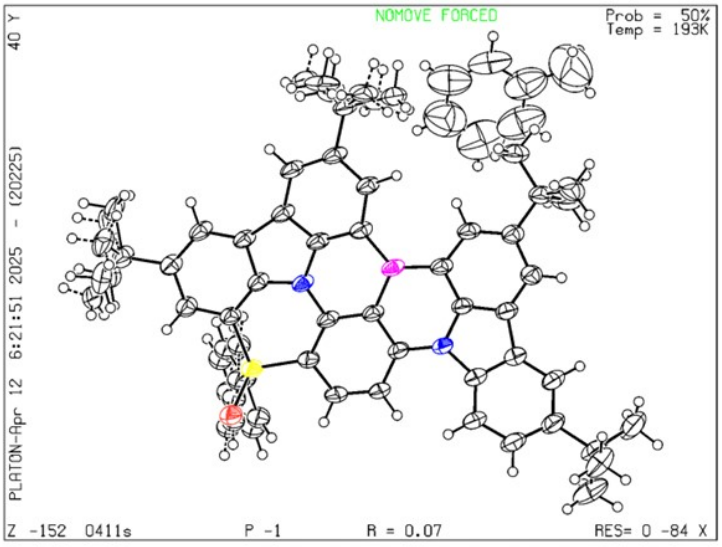

Fig. S17 Single-crystal structure of NBNPS.

Table S3. X-Ray Crystallographic Data and Structure Refinement for NBNPS.

Compound	NBNPS
CCDC No.	2452670
Formula	$C_{52}H_{52}BN_2SP$
Formula weight	778.85
T (K)	193.00
Wavelength (Å)	0.71073
Crystal system	Triclinic
Space group	$P\bar{1}$
a (Å)	11.4849(10)
b (Å)	14.1923(10)
c (Å)	16.0109(11)
α (deg)	66.987(2)
β (deg)	69.582(2)
γ (deg)	75.458(2)
V (Å^3)	2231.1(3)
Z	1
ρ_{calcd} (mg m^{-3})	1.228
μ (Mo Kα) (mm^{-1})	0.834
F (000)	878.0
Radiation	MoKα (λ = 1.34139)
2Θ range for data collection/°	9.302 to 105.962
Reflns collected	26918
Index ranges	-13 ≤ h ≤ 13 -15 ≤ k ≤ 16 -19 ≤ l ≤ 19
Independent reflections	7821 [R_{int} = 0.1876, R_{sigma} = 0.1143]
Data/restraints/params	7821/389/670
GOF on F^2	1.050
R_1[a], wR_2[b][$I > 2\sigma(I)$]	0.0657, 0.1672
R_1[a], wR_2[b](all data)	0.0993,0.1925
Largest diff. peak/hole / e Å^{-3}	0.56/-0.45

R_1[a] = $\sum||F_o|-|F_c||/\sum|F_o|$. wR_2[b] = $[\sum w(F_o^2-F_c^2)^2/\sum w(F_o^2)]^{1/2}$

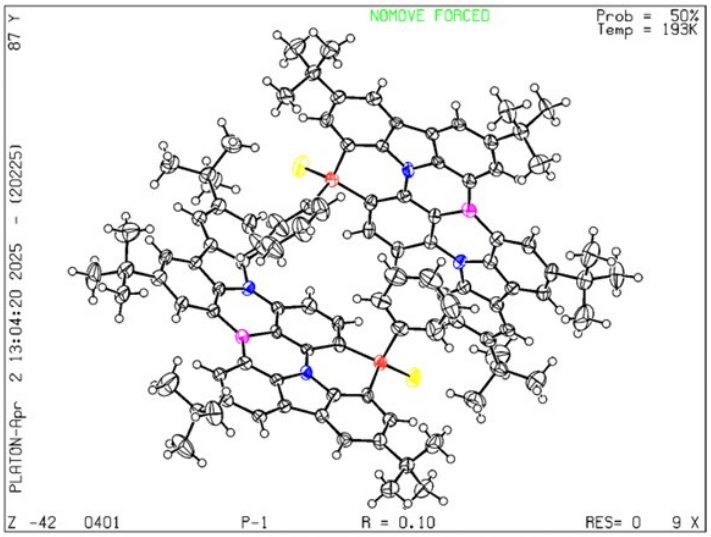

Fig. S18 Single-crystal structure of NBNPS.

Table S4. X-Ray Crystallographic Data and Structure Refinement for NBNPSe.

Compound	NBNPO
CCDC No.	2452672
Formula	$C_{52}H_{52}BN_2PSe$
Formula weight	825.76
T (K)	193.00
Wavelength (Å)	0.71073
Crystal system	Triclinic
Space group	$P\bar{1}$
a (Å)	11.912(3)
b (Å)	19.904(4)
c (Å)	21.598(4)
α (deg)	105.673(6)
β (deg)	93.452(7)
γ (deg)	106.204(7)
V (Å^3)	4683.5(16)
Z	1
ρ_{calcd} (mg m^{-3})	1.291
μ (Mo Kα) (mm^{-1})	0.988
F (000)	1896.0
Radiation	MoKα (λ = 0.71073)
2Θ range for data collection/°	3.846 to 50.054
Reflns collected	16452
Index ranges	-14 ≤ h ≤ 14 -23 ≤ k ≤ 22 0 ≤ l ≤ 25
Independent reflections	16452 [R_{int} = -, R_{sigma} = 0.2044]
Data/restraints/params	16452/793/1040
GOF on F^2	1.031
R_1[a], wR_2[b][$I > 2\sigma(I)$]	0.1039, 0.2044
R_1[a], wR_2[b](all data)	0.1784, 0.3255
Largest diff. peak/hole / e Å^{-3}	1.30/-1.50

R_1[a] = $\sum||F_o|-|F_c||/\sum|F_o|$. wR_2[b] = $[\sum w(F_o^2-F_c^2)^2/\sum w(F_o^2)]^{1/2}$

6. Photophysical property

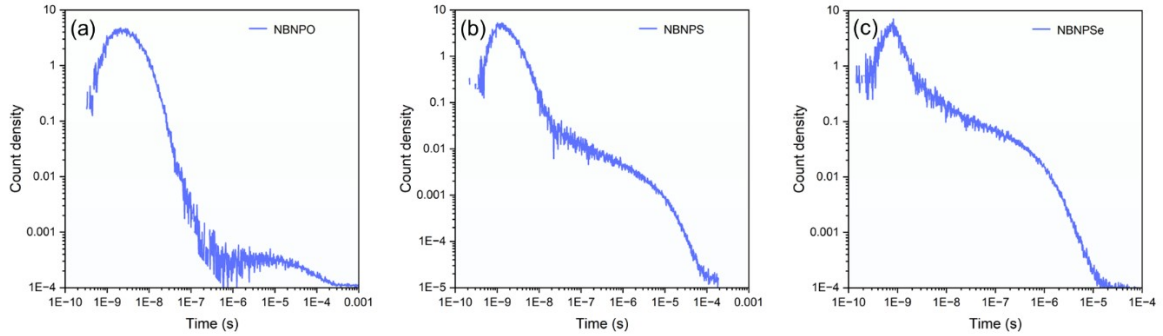

Fig. S19 Transient PL prompt and transient PL prompt and decay curves of NBNPO, NBNPS and NBNPSe (5 wt.% in mCBP, 20 nm).

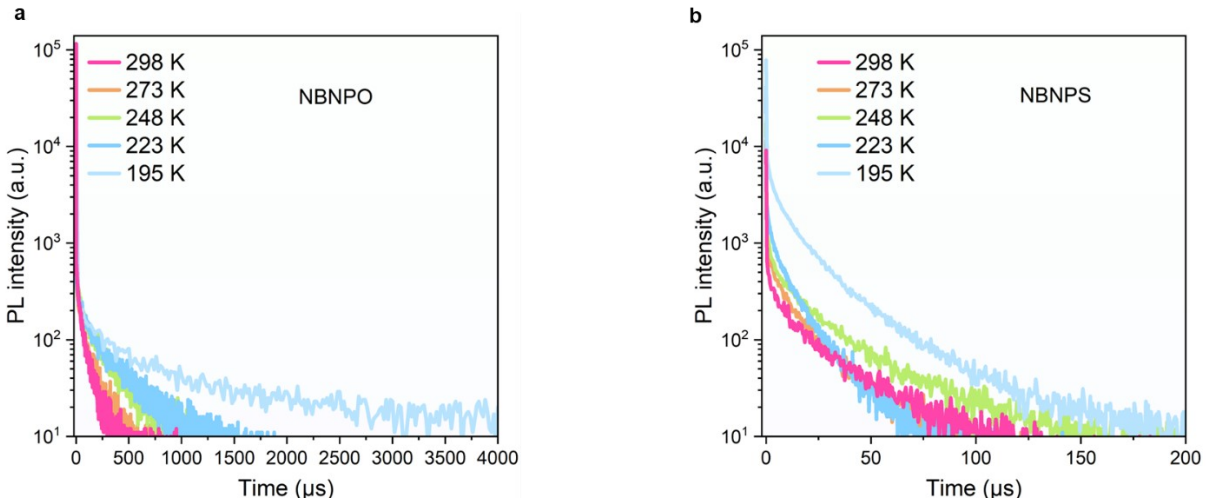

Fig. S20 Variable-temperature transient PL decay curves of NBNPO or NBNPS in 5 wt.% doped films with mCBP host.

Table S5. The detailed decay lifetimes, percentage contributions of prompt and delayed fluorescence, and rate constants at various temperatures in doped film (NBNPO in 5 wt.% doped films with mCBP host.).

Temperature	τ_p (ns)	τ_d (μs)	PF (%)	DF (%)	k_{RISC} (10^4 s^{-1})
298 K	5.70	43	0.21	0.79	10.8
273 K	5.59	76	0.24	0.76	5.4
248 K	5.61	149	0.32	0.68	2.0
223 K	5.72	175	0.39	0.61	1.4
195 K	5.65	511	0.38	0.62	0.5

Table S6. The detailed decay lifetimes, percentage contributions of prompt and delayed fluorescence, and rate constants at various temperatures in doped film (NBNPS in 5 wt.% doped films with mCBP host.).

Temperature	τ_p (ns)	τ_d (μs)	PF (%)	DF (%)	k_{RISC} (10^4 s^{-1})
298 K	1.97	7.22	0.31	0.69	43.7
273 K	2.01	12.12	0.32	0.68	25.2
248 K	1.86	18.75	0.34	0.66	15.3
223 K	1.71	21.47	0.35	0.65	13.0
195 K	1.81	42.74	0.38	0.62	6.0

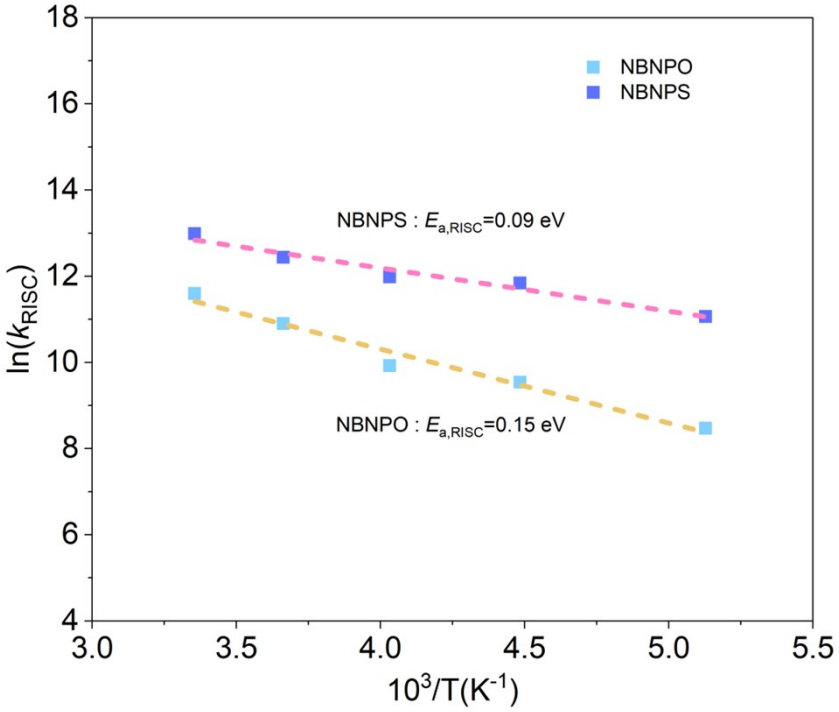

Fig. S21 Arrhenius plots of the rate constants for RISC (k_{RISC}) measured for NBNPO and NBNPS doped films under vacuum. ΔE_{ST} denotes activation energy for RISC process from S_1 to T_1 states.

7. Theoretical calculation

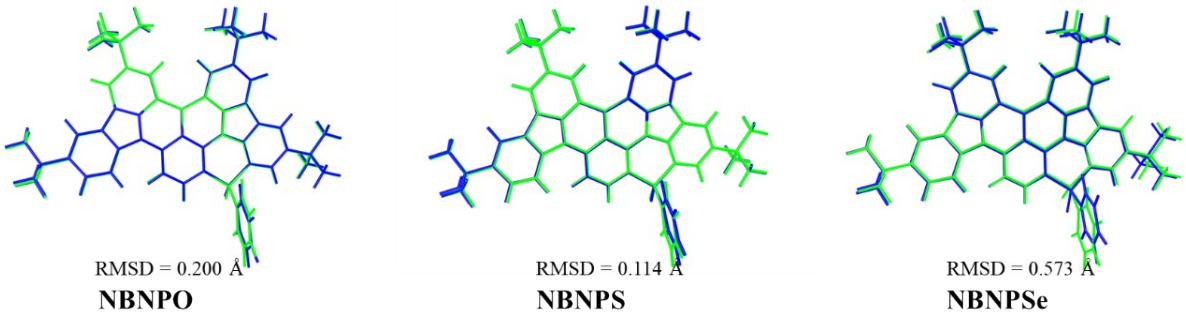

Fig. S22 The theoretically calculated emission spectra in toluene solution, with the inset showing the optimized structures of the S_0 (blue) and S_1 (green) states, along with their corresponding RMSD values.

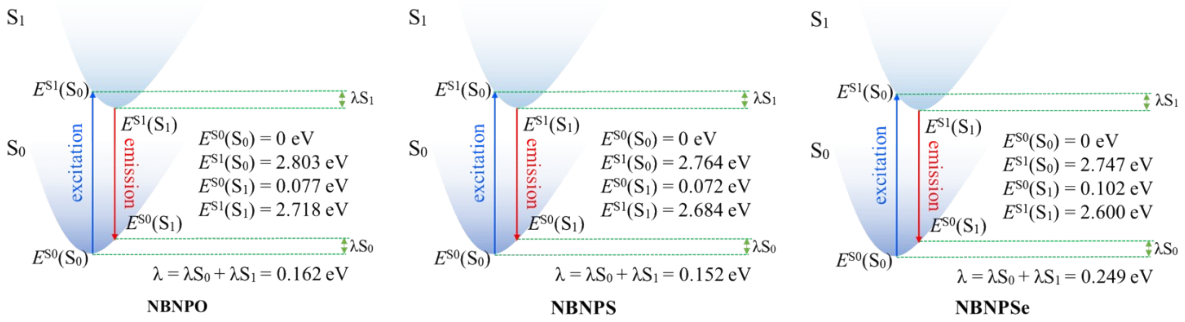

Fig. S23 The optimized S_0 and S_1 structures and reorganization energy of NBNPO, NBNPS, and NBNPSe.

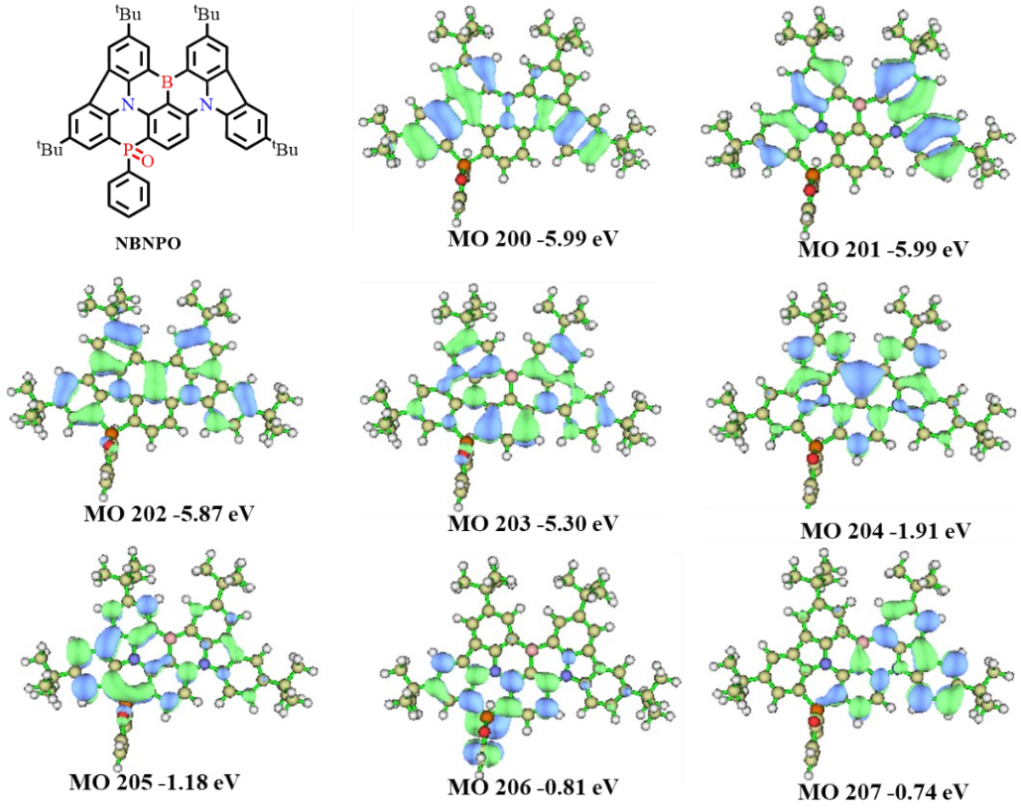

Fig. S24 Electronic cloud distributions of NBNPO in selected orbitals.

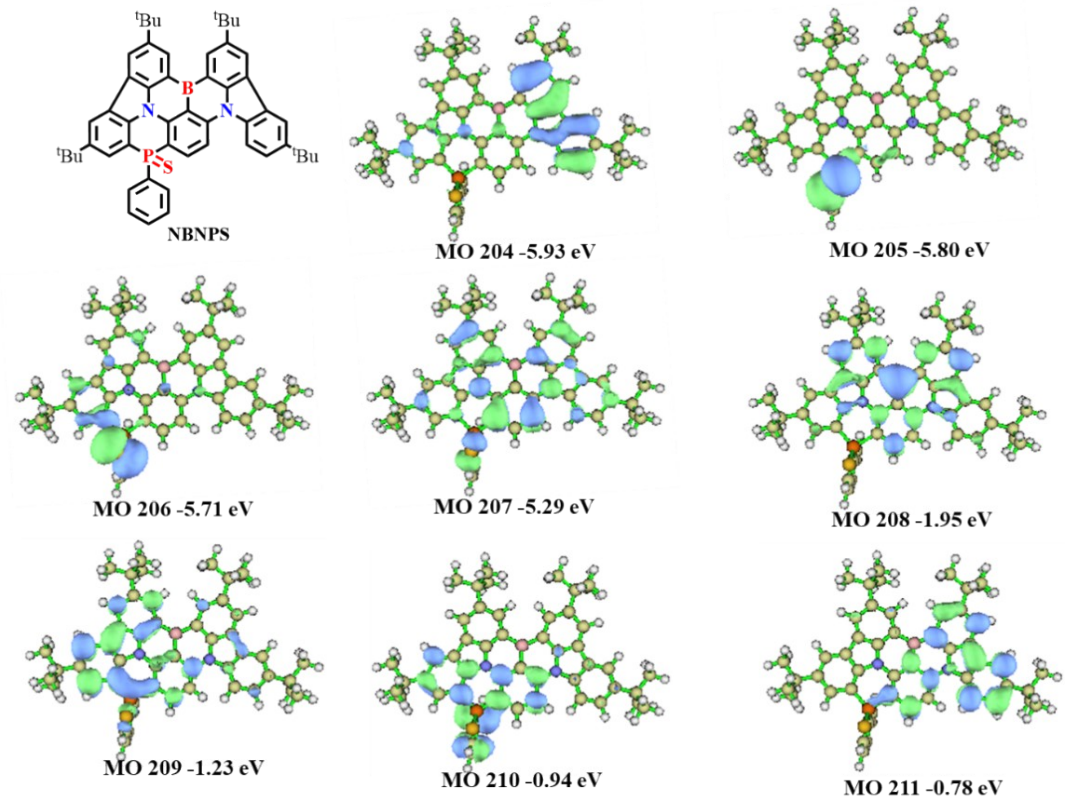

Fig. S25 Electronic cloud distributions of NBNPS in selected orbitals.

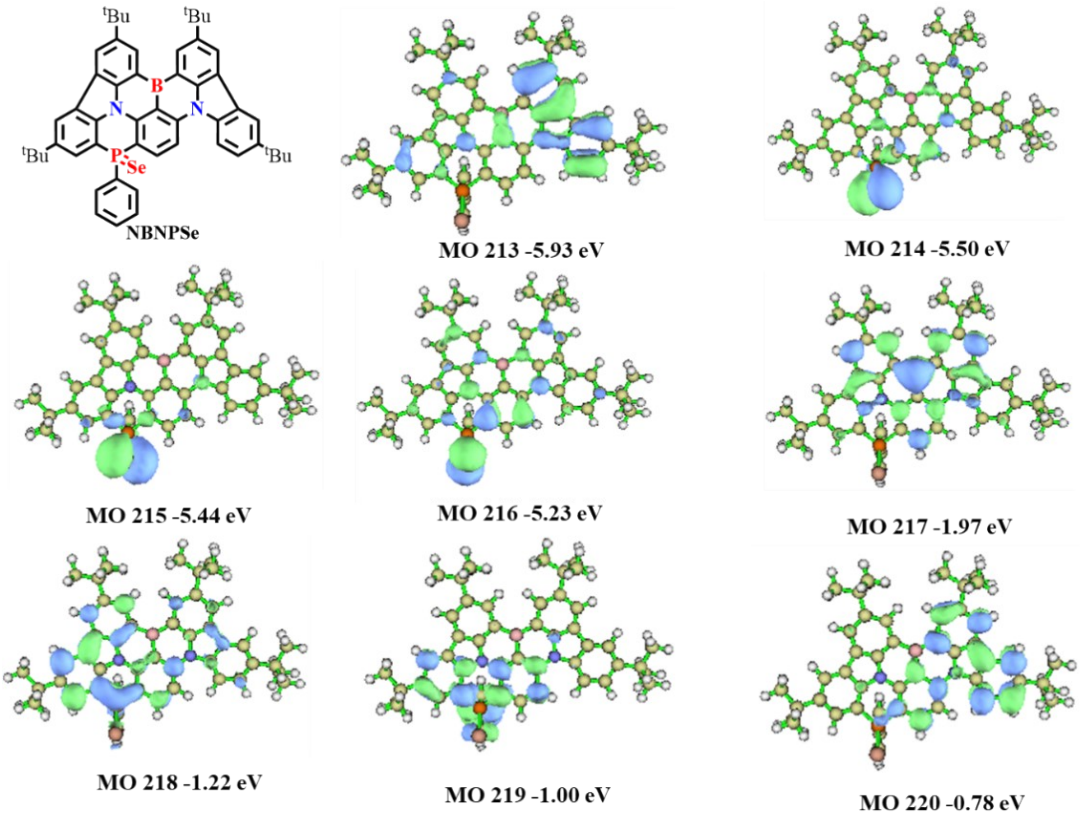

Fig. S26 Electronic cloud distributions of NBNPSe in selected orbitals.

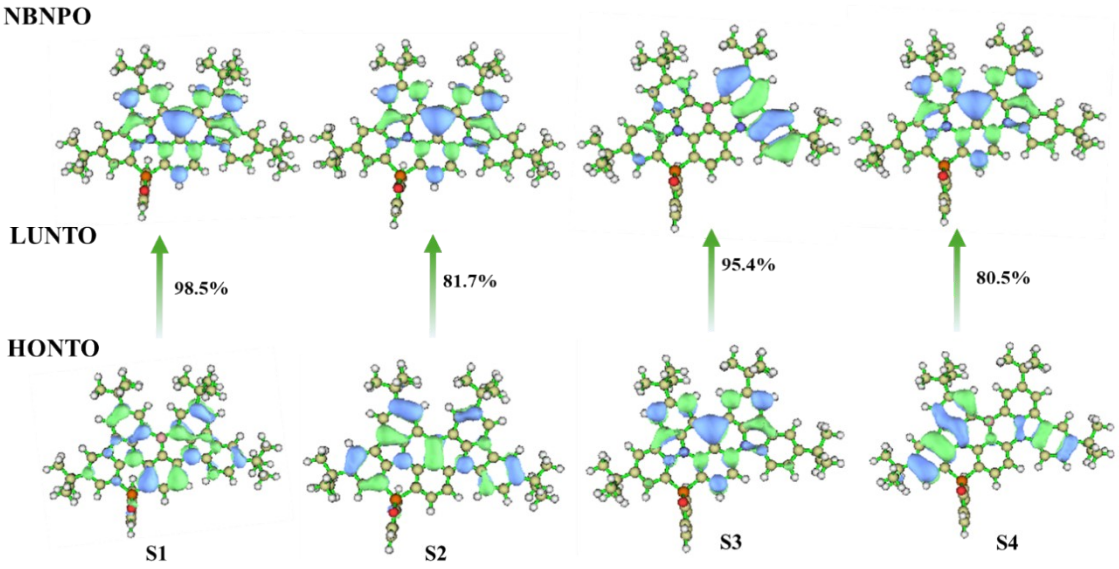

Fig. S27 Natural transition orbital (NTO) analysis for $S_0 \rightarrow S_n$ transition of NBNPO.

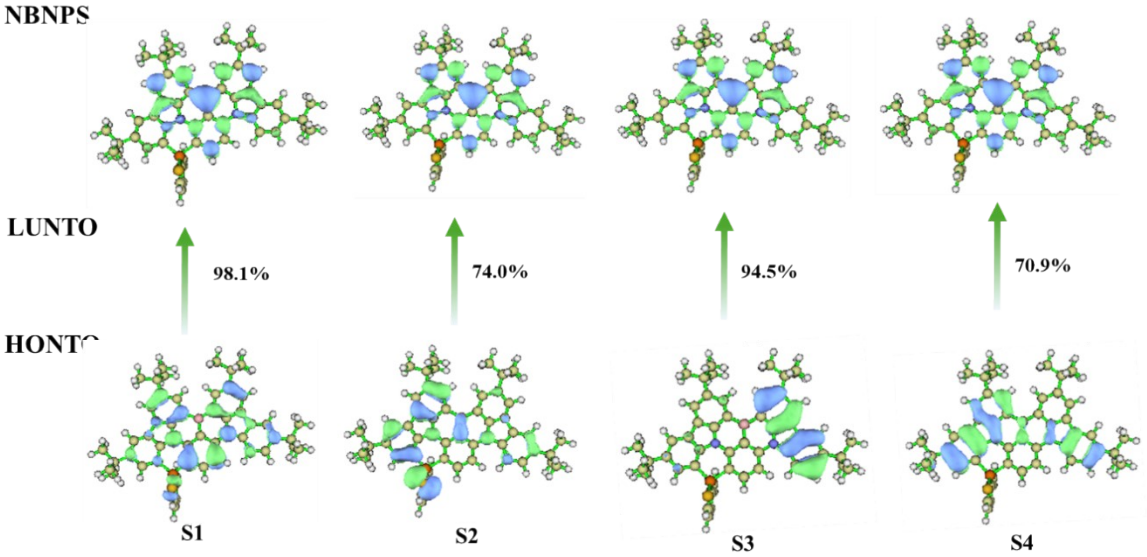

Fig. S28 Natural transition orbital (NTO) analysis for $S_0 \rightarrow S_n$ transition of NBNPS.

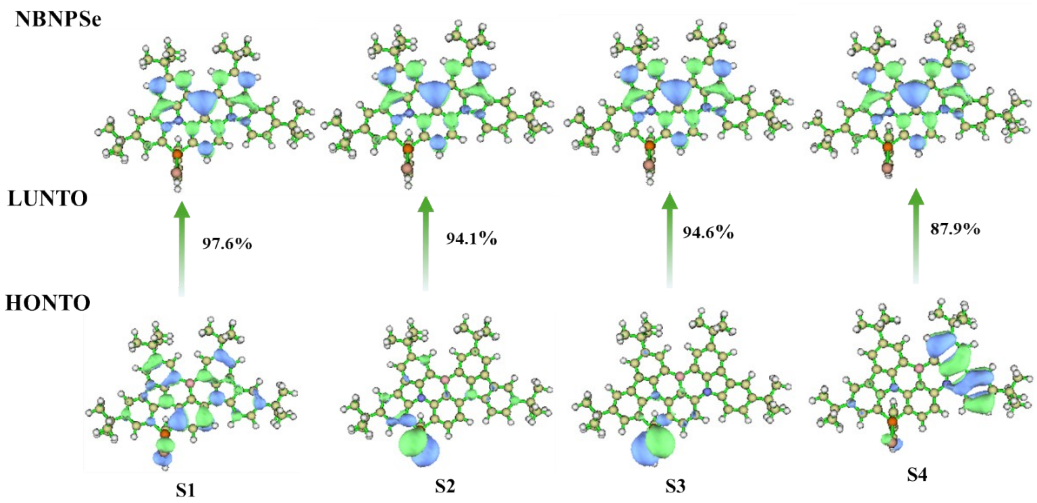

Fig. S29 Natural transition orbital (NTO) analysis for $S_0 \rightarrow S_n$ transition of NBNPSe.

Table S7. Analysis of excited states (1-4) according to MO-MO contributions of NBNPO.

NBNPO			
S_1	2.8363 eV	437.13 nm	f = 0.4977
203 → 204 0.70173			
S_2	3.3994 eV	364.73 nm	f = 0.0133
201→ 204 0.21744 202 → 204 0.60115 203 → 205 0.26378			
S_3	3.4327 eV	361.18 nm	f = 0.0208
201 → 204 0.64628 202 → 204 -0.24332			
S_4	3.5033 eV	353.91 nm	f = 0.0056
200 → 204 0.63428 203 → 205 -0.27176			

Table S8. Analysis of excited states (1-4) according to MO-MO contributions of NBNPS.

NBNPS			
S_1	2.9041 eV	426.92 nm	f = 0.5277
207 → 208 0.70047			
S_2	3.4779 eV	356.49 nm	f = 0.0125
206 → 208 0.60854 207 →209 -0.29527			
S_3	3.5428 eV	349.96 nm	f = 0.0242
205 → 208 0.68738			
S_4	3.6342 eV	341.16 nm	f = 0.0066
202 → 208 -0.16865 203 → 208 0.14080 204 → 208 0.55344 207 → 209 -0.32760			

Table S9. Analysis of excited states (1-4) according to MO-MO contributions of NBNPSe.

NBNPSe			
S_1	2.8851 eV	429.75 nm	f = 0.5013
216 → 217 0.69850			
S_2	3.3916 eV	365.57 nm	f = 0.0203
212 → 217 -0.12978 214 → 217 0.11855 215 → 217 0.66314 216 → 218 -0.11599			
S_3	3.4490 eV	359.48 nm	f = 0.0217
212 → 217 -0.12066 214 → 217 0.65906 215 → 217 -0.15587 216 → 218 -0.10550			
S_4	3.5290 eV	351.33 nm	f = 0.0156
213 → 217 0.65402 215 → 217 0.10915 216 → 218 0.20059			

Table S10. Spin-orbit coupling (SOC) matrix elements computed with PySOC.

	NBNPO (cm^{-1})	NBNPS (cm^{-1})	NBNPSe (cm^{-1})
SOC ($<S_1\|\hat{H}_{SOC}\|T_1>$)	0.06	0.71	6.23
SOC ($<S_1\|\hat{H}_{SOC}\|T_2>$)	0.26	2.92	15.59
SOC ($<S_1\|\hat{H}_{SOC}\|T_3>$)	0.34	2.76	17.19

Table S11. Cartesian coordinates (Å) and transition sates of optimized NBNPO structure in the ground state (S_0) calculated at the b3lyp/6-31g(d,p) level of theory.

	X	Y	Z
C	1.73998500	4.25599800	0.49654500
C	2.97034400	3.59088900	0.33221400
C	2.99522300	2.22505700	0.05595900
C	1.76223300	1.54904300	-0.05843100
C	0.50220800	2.14135500	0.06873600
C	0.54636600	3.52022000	0.36450000
C	4.03613000	1.22446400	-0.15591600
C	3.36640300	0.00140300	-0.38320300
N	1.99052200	0.20630300	-0.31888600
C	5.43163300	1.23551200	-0.17182500
C	6.15164600	0.05201500	-0.40907500
C	5.43484000	-1.14131100	-0.62962400
C	4.03516400	-1.19592300	-0.61692000
C	1.00291200	-0.75755500	-0.44657300
C	1.36695200	-2.09567200	-0.70430400
C	0.32171300	-3.01462800	-0.87274400
C	-1.01011400	-2.65839900	-0.73499900
C	-1.35509700	-1.33249800	-0.41516700

C	-0.35014300	-0.32520800	-0.31174700
C	1.66404300	5.76413800	0.81635000
C	7.69310600	0.01587900	-0.43575500
C	8.20519200	-0.95810100	0.65213700
C	8.17400400	-0.46771700	-1.82464900
C	8.31568400	1.39934400	-0.16797100
C	3.05720100	6.41465800	0.91553500
C	0.94246000	5.97189400	2.16919800
C	0.87795500	6.49128000	-0.30065100
B	-0.69890400	1.17625800	-0.12802500
N	-2.68676600	-0.95074600	-0.22970300
C	-3.87043000	-1.73090000	-0.13059200
C	-4.98634600	-0.85951800	-0.13033200
C	-4.47145700	0.49653500	-0.18391600
C	-3.06560400	0.39318300	-0.20742200
C	-5.05271300	1.75783500	-0.19670600
C	-4.24662700	2.91546800	-0.22585600
C	-2.85463700	2.75560000	-0.21675000
C	-2.20661400	1.49773900	-0.19216400
C	-4.07161200	-3.10322400	0.03818400
C	-5.37886600	-3.57581500	0.13654600
C	-6.51003800	-2.73589500	0.08881900
C	-6.28636000	-1.36164900	-0.03304800
C	-4.92582500	4.29928900	-0.25995100
C	-5.80641900	4.41033700	-1.52736000
C	-5.81248200	4.47102900	0.99642100
C	-3.90799400	5.45565900	-0.28497400
C	-7.91948500	-3.34751200	0.19166400
C	-8.05740200	-4.11307700	1.52911700
C	-8.14148400	-4.32783200	-0.98451200
C	-9.02514500	-2.27643100	0.13785300
P	3.07186900	-2.69412300	-0.96210000
C	3.41608900	-3.85258300	0.41319300
C	3.86393400	-5.13916100	0.08842000
C	4.14411800	-6.05958500	1.10023500
C	3.97909900	-5.69909000	2.43805100
C	3.53268700	-4.41622400	2.76762400
C	3.25160000	-3.49597400	1.75941400
O	3.32589800	-3.35420100	-2.28820600
H	3.90420100	4.13274600	0.42469900
H	-0.39153400	4.04223300	0.51450100

H	5.95439800	2.16850300	0.00222000
H	5.97917300	-2.06030600	-0.82219100
H	0.56217200	-4.04075000	-1.13573300
H	-1.77085100	-3.39671000	-0.93244700
H	9.30026400	-0.99638200	0.64329800
H	7.88440400	-0.63628700	1.64832700
H	7.83673600	-1.97599800	0.49585900
H	9.26871000	-0.50498200	-1.85572800
H	7.83388100	0.20951600	-2.61463200
H	7.80008200	-1.46789500	-2.06091500
H	9.40716800	1.32211500	-0.19575100
H	8.03888800	1.78849600	0.81754500
H	8.01977500	2.13461000	-0.92349600
H	3.66110200	5.96898300	1.71286300
H	2.95018000	7.48023200	1.14208400
H	3.61400700	6.33285100	-0.02377200
H	1.48301800	5.47569700	2.98180300
H	0.87727000	7.03976500	2.40656300
H	-0.07572600	5.57247100	2.15434200
H	1.36489900	6.35770400	-1.27205800
H	0.82351200	7.56574100	-0.09202800
H	-0.14666100	6.11846700	-0.38773700
H	-6.13489900	1.84837900	-0.18853300
H	-2.23209300	3.63912100	-0.24397400
H	-3.25425000	-3.80280400	0.13652700
H	-5.51543900	-4.64489600	0.26505300
H	-7.11592700	-0.66426400	-0.03981400
H	-6.58322600	3.64031700	-1.55309600
H	-6.30422400	5.38592000	-1.56276000
H	-5.20200200	4.30395600	-2.43397000
H	-5.21350900	4.40349100	1.91043100
H	-6.59372400	3.70712900	1.05342900
H	-6.30595100	5.44937200	0.98465500
H	-3.27072700	5.45764600	0.60554400
H	-3.26390600	5.41435400	-1.16944900
H	-4.43959700	6.41231700	-0.31002700
H	-9.05816700	-4.55092200	1.61577900
H	-7.90441300	-3.44300200	2.38127400
H	-7.33183900	-4.92768800	1.61135700
H	-9.13729300	-4.78075300	-0.92101600
H	-8.06432700	-3.80972600	-1.94587500

H	-7.40676800	-5.13845300	-0.98301200
H	-10.00660700	-2.75610500	0.20727500
H	-8.94684300	-1.56646400	0.96785500
H	-9.00058000	-1.71179400	-0.79999900
H	3.98603000	-5.39954400	-0.95841800
H	4.49086000	-7.05646100	0.84354600
H	4.19738100	-6.41537200	3.22506400
H	3.40384700	-4.13516800	3.80883700
H	2.90397900	-2.50021500	2.02162200

Table S12. Cartesian coordinates (Å) and transition sates of optimized NBNPS structure in the ground state (S_0) calculated at the b3lyp/6-31g(d,p) level of theory.

	X	Y	Z
C	1.64409500	4.31967000	0.47598700
C	2.88006300	3.66435400	0.31572700
C	2.91705300	2.29386800	0.06506300
C	1.69069100	1.60259600	-0.02634400
C	0.42531800	2.18581300	0.08936900
C	0.45737000	3.57015100	0.36026900
C	3.96753200	1.30283700	-0.14268100
C	3.30955600	0.06783600	-0.33624500
N	1.93184300	0.25723600	-0.26083200
C	5.36247800	1.33320100	-0.18527700
C	6.09374300	0.15731200	-0.42307300
C	5.39015300	-1.04960500	-0.61101800
C	3.99388300	-1.12086700	-0.56238500
C	0.95279800	-0.71432400	-0.39652900
C	1.32317300	-2.05141500	-0.64944600
C	0.28775000	-2.97355000	-0.84934100
C	-1.04713500	-2.62353800	-0.73129800
C	-1.40323200	-1.30278400	-0.40318500
C	-0.40535300	-0.29009800	-0.28388400
C	1.55478200	5.83184700	0.77225400
C	7.63429500	0.14147500	-0.48630500
C	8.18484100	-0.81274900	0.60032900
C	8.08751900	-0.35258800	-1.88084900
C	8.24369400	1.53634100	-0.24954900
C	2.94211500	6.49684300	0.85572200
C	0.83672700	6.05313300	2.12483300
C	0.75745200	6.53455000	-0.35236100
B	-0.76703000	1.20971400	-0.10601300

N	-2.73864100	-0.93134000	-0.22992400
C	-3.91673100	-1.72137200	-0.14115800
C	-5.03918500	-0.85873000	-0.14440200
C	-4.53452700	0.50156700	-0.18992200
C	-3.12777300	0.40937000	-0.20496000
C	-5.12531800	1.75829900	-0.20162400
C	-4.32773200	2.92206900	-0.22179400
C	-2.93472700	2.77288000	-0.20487900
C	-2.27686400	1.51994600	-0.18055300
C	-4.10754500	-3.09581600	0.02148300
C	-5.41155700	-3.57900500	0.11093100
C	-6.54907000	-2.74784700	0.05980000
C	-6.33569700	-1.37145000	-0.05627500
C	-5.01719300	4.30085100	-0.25431400
C	-5.89419000	4.40912300	-1.52446000
C	-5.90947700	4.46193300	0.99949800
C	-4.00789400	5.46482500	-0.27240000
C	-7.95413800	-3.37105400	0.15258800
C	-8.09302800	-4.14329100	1.48610200
C	-8.16178600	-4.34816800	-1.02887900
C	-9.06798200	-2.30852100	0.09733400
P	3.04684700	-2.65826800	-0.78634600
C	3.33071900	-3.62300600	0.76076000
C	3.86809900	-4.91240500	0.69724300
C	4.09252000	-5.63509900	1.87066900
C	3.78173600	-5.07452700	3.10958300
C	3.24373200	-3.78670200	3.17783700
C	3.01853200	-3.06264000	2.00889200
S	3.45847100	-3.68798600	-2.42240900
H	3.80892100	4.21743600	0.39053100
H	-0.48484500	4.08660600	0.50139500
H	5.87522000	2.27602400	-0.03652800
H	5.93914100	-1.96351600	-0.81300900
H	0.54129700	-3.99257600	-1.12671400
H	-1.80125600	-3.36276400	-0.95011000
H	9.27972100	-0.83729900	0.56536700
H	7.88399800	-0.48307600	1.60018100
H	7.82589300	-1.83696900	0.46476200
H	9.18155200	-0.37521800	-1.93824600
H	7.71890800	0.31038000	-2.67015200
H	7.72186200	-1.36041900	-2.09628500

H	9.33514500	1.47328900	-0.30196900
H	7.98436700	1.93352700	0.73751800
H	7.92041800	2.25824000	-1.00675900
H	3.55357700	6.06872500	1.65689200
H	2.82598000	7.56460600	1.06681500
H	3.49562200	6.40640500	-0.08474400
H	1.38568300	5.57498800	2.94261700
H	0.76170700	7.12380300	2.34596700
H	-0.17740200	5.64323100	2.12046100
H	1.24226800	6.39187500	-1.32353400
H	0.69299000	7.61130600	-0.15906300
H	-0.26373300	6.15052400	-0.43026000
H	-6.20817200	1.84066800	-0.19946400
H	-2.31962400	3.66160200	-0.22504900
H	-3.28500400	-3.78914500	0.12133900
H	-5.54037700	-4.64957700	0.23480500
H	-7.17072200	-0.68067300	-0.06543100
H	-6.66543200	3.63372300	-1.55502300
H	-6.39886200	5.38118900	-1.55873300
H	-5.28599500	4.30970100	-2.42932600
H	-5.31303500	4.39720000	1.91536600
H	-6.68420900	3.69112700	1.05177100
H	-6.41126500	5.43602600	0.98848500
H	-3.37389500	5.46902200	0.62044900
H	-3.36039000	5.43069500	-1.15470800
H	-4.54644300	6.41758700	-0.29671100
H	-9.09080900	-4.58918900	1.56558600
H	-7.94978600	-3.47567200	2.34188100
H	-7.36165100	-4.95264000	1.56880400
H	-9.15405400	-4.80968600	-0.97247900
H	-8.08400100	-3.82537000	-1.98764700
H	-7.42023200	-5.15249800	-1.02683600
H	-10.04592100	-2.79636400	0.15904900
H	-9.00007200	-1.60179900	0.93100900
H	-9.04272600	-1.73948800	-0.83784000
H	4.10203900	-5.33735500	-0.27421900
H	4.50903000	-6.63656700	1.81428700
H	3.95621500	-5.63840900	4.02143900
H	2.99892500	-3.34763200	4.14052900
H	2.59819800	-2.06290200	2.07133700

Table S13. Cartesian coordinates (Å) and transition sates of optimized NBNPSe structure in the ground state (S_0) calculated at the b3lyp/6-31g(d,p) level of theory.

	X	Y	Z
C	-4.31060000	2.32810000	-0.56300000
C	-4.72480000	1.35190000	-1.39640000
C	-4.03320000	0.20860000	-1.46890000
C	-2.94160000	-0.02080000	-0.73080000
C	-2.53370000	0.92640000	0.11610000
C	-3.20680000	2.08560000	0.17650000
C	-4.18450000	-0.89680000	-2.20120000
C	-3.16620000	-1.69690000	-1.85140000
N	-2.41460000	-1.16300000	-0.96020000
C	-5.10190000	-1.23310000	-3.11660000
C	-5.02540000	-2.42750000	-3.73660000
C	-4.00080000	-3.23330000	-3.38850000
C	-3.08960000	-2.88260000	-2.46690000
C	-1.35190000	-1.63350000	-0.40930000
C	-0.86690000	-2.84570000	-0.74310000
C	0.25530000	-3.29570000	-0.17060000
C	0.90250000	-2.55480000	0.73660000
C	0.49610000	-1.33550000	1.14030000
C	-0.65180000	-0.94340000	0.52640000
C	-5.03730000	3.67370000	-0.43400000
C	-6.03420000	-2.88150000	-4.79860000
C	-5.29330000	-3.14060000	-6.12940000
C	-6.72480000	-4.18030000	-4.32660000
C	-7.14720000	-1.84800000	-5.08600000
C	-6.29670000	3.79100000	-1.32280000
C	-4.07920000	4.81500000	-0.84140000
C	-5.49040000	3.87670000	1.02970000
B	-1.26100000	0.46420000	0.94430000
N	1.10310000	-0.62240000	2.03370000
C	2.21070000	-0.78600000	2.68210000
C	2.41460000	0.21730000	3.55810000
C	1.38080000	1.04640000	3.42900000
C	0.62940000	0.48830000	2.47570000
C	1.06650000	2.18700000	4.05550000
C	-0.07370000	2.83320000	3.74410000
C	-0.83320000	2.28050000	2.77810000
C	-0.48740000	1.14770000	2.14720000
C	3.20880000	-1.69060000	2.67710000

C	4.27090000	-1.59670000	3.49690000
C	4.43350000	-0.59460000	4.37970000
C	3.46220000	0.33400000	4.38530000
C	-0.45360000	4.13330000	4.46420000
C	-0.59530000	3.85550000	5.97700000
C	0.65170000	5.18710000	4.23040000
C	-1.78620000	4.75460000	3.98380000
C	5.66520000	-0.53540000	5.29000000
C	6.93980000	-0.45020000	4.42180000
C	5.71630000	-1.80720000	6.16530000
C	5.67690000	0.67960000	6.24580000
P	-1.68910000	-3.93610000	-1.97860000
C	-0.61710000	-4.24390000	-3.44180000
C	-0.94730000	-5.17510000	-4.35430000
C	-0.16930000	-5.38810000	-5.42720000
C	0.94570000	-4.66350000	-5.60400000
C	1.27420000	-3.72180000	-4.70700000
C	0.49350000	-3.51090000	-3.63560000
Se	-2.31110000	-5.56050000	-1.12330000
H	-5.61010000	1.46640000	-2.03610000
H	-2.84600000	2.87000000	0.84850000
H	-5.89960000	-0.51250000	-3.34170000
H	-3.89190000	-4.21700000	-3.87010000
H	0.65610000	-4.29040000	-0.43400000
H	1.77210000	-3.07290000	1.13860000
H	-6.00020000	-3.44260000	-6.93490000
H	-4.76250000	-2.22380000	-6.47380000
H	-4.53950000	-3.95470000	-6.05210000
H	-7.48830000	-4.52360000	-5.06080000
H	-7.24120000	-4.02430000	-3.35200000
H	-6.01250000	-5.02470000	-4.19700000
H	-7.85520000	-2.22080000	-5.86060000
H	-6.73450000	-0.89020000	-5.47630000
H	-7.75940000	-1.63410000	-4.18070000
H	-6.05110000	3.70780000	-2.40570000
H	-6.79390000	4.77890000	-1.19220000
H	-7.05910000	3.02100000	-1.06600000
H	-3.71550000	4.67510000	-1.88500000
H	-4.58460000	5.80590000	-0.79120000
H	-3.18650000	4.88470000	-0.18160000
H	-6.15640000	3.04640000	1.35810000

H	-6.05530000	4.82860000	1.15100000
H	-4.63960000	3.92690000	1.74440000
H	1.73660000	2.58240000	4.83190000
H	-1.76900000	2.76300000	2.48890000
H	3.26430000	-2.55320000	2.00770000
H	5.04330000	-2.38060000	3.42450000
H	3.51240000	1.19880000	5.05990000
H	0.35320000	3.50510000	6.44020000
H	-0.89660000	4.77300000	6.53140000
H	-1.36970000	3.07770000	6.16720000
H	0.79110000	5.38200000	3.14260000
H	1.63630000	4.87730000	4.64470000
H	0.39760000	6.15640000	4.71600000
H	-1.75510000	5.02660000	2.90420000
H	-2.65060000	4.07440000	4.15800000
H	-2.01530000	5.69490000	4.53460000
H	7.85520000	-0.37640000	5.05150000
H	6.91220000	0.44670000	3.76160000
H	7.07640000	-1.34170000	3.77100000
H	6.58440000	-1.78550000	6.86240000
H	4.79290000	-1.90360000	6.78100000
H	5.81840000	-2.73820000	5.56560000
H	6.58410000	0.67750000	6.89160000
H	5.69180000	1.64520000	5.69150000
H	4.80210000	0.67390000	6.93490000
H	-1.86270000	-5.77900000	-4.24140000
H	-0.44870000	-6.15640000	-6.16760000
H	1.58430000	-4.83510000	-6.48650000
H	2.18450000	-3.11650000	-4.85400000
H	0.78370000	-2.72200000	-2.92270000

8. Device performances of NBNPO, NBNPS and NBNPSe.

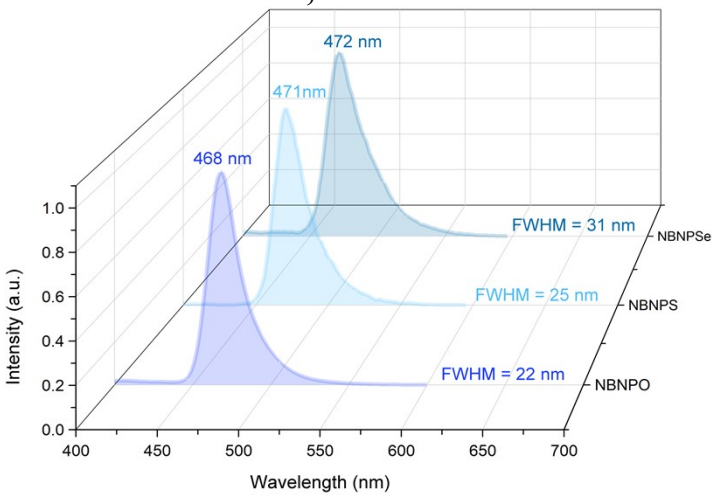

Fig. S30 Normalized PL spectra in doped films (5 wt.% in mCBP).

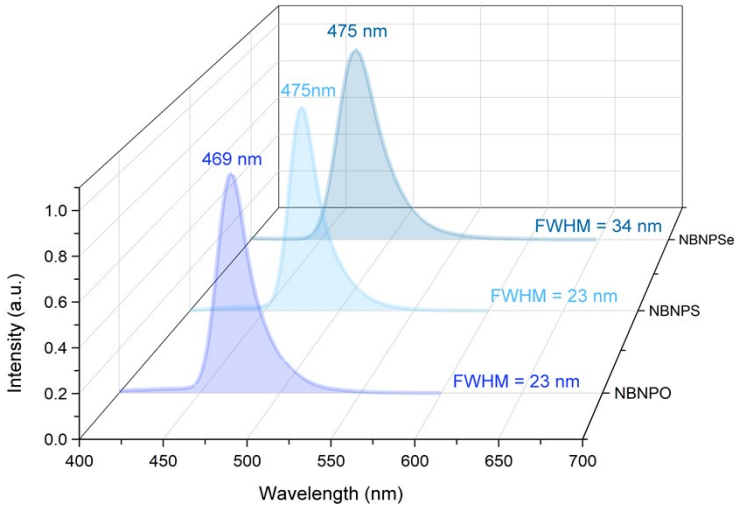

Fig. S31 Normalized PL spectra in doped films (mCBP: 20 wt% m4TCzPhBN: 5 wt.% NBNPX (X = O, S, Se)).

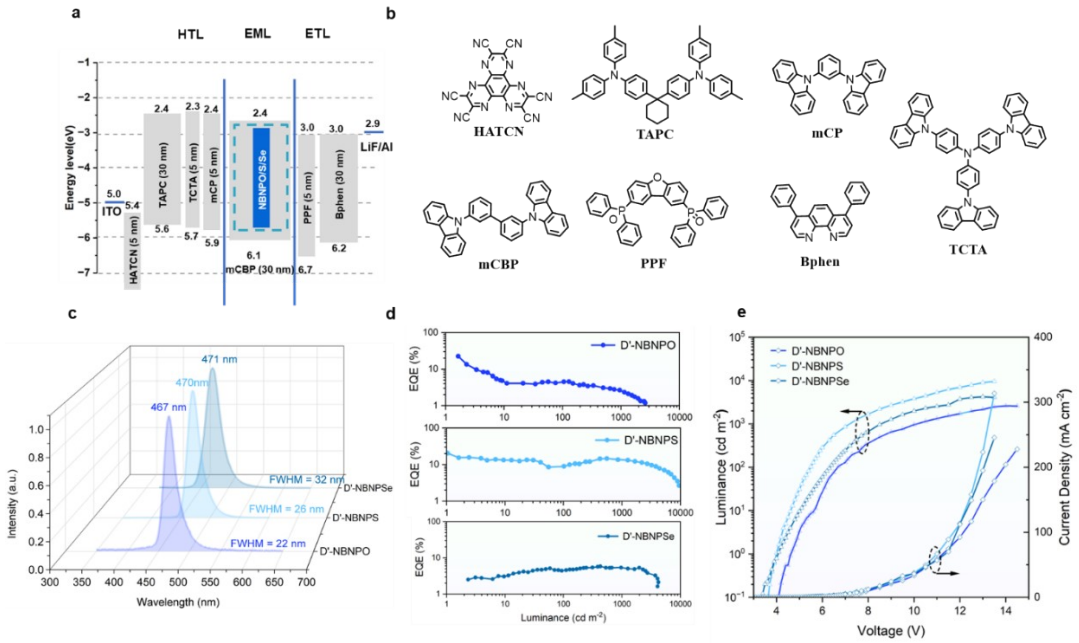

Fig. S32 Device architecture, molecular structures of materials and device performances of the unoptimized NBNPX (X = O, S, Se)-based OLEDs.

Table S14. Device performance data of the unoptimized NBNPX (X = O, S, Se)-based OLEDs.

Device	$V_{turn\text{-}on}$ [a] [V]	λ_{EL} [b] [nm]	FWHM [nm/eV]	L_{max} [c] [cd m^{-2}]	$CE_{max/100/1000}$ [d] [cd A^{-1}]	$EQE_{max/100/1000}$ [e] [%]	PE_{max} [f] [lm W^{-1}]
D'-NBNPO	4.5	467	22/0.13	2686	23.95/4.79/2.83	22.4/4.5/2.3	15.67/2.24/0.75
D'-NBNPS	3.9	470	26/0.15	9487	23.27/11.98/11.80	20.5/10.6/10.4	18.26/10.58/10.46
D'-NBNPSe	4.0	471	32/0.18	4086	5.06/4.70/5.17	5.2/4.6/5.1	3.12/2.31/1.80

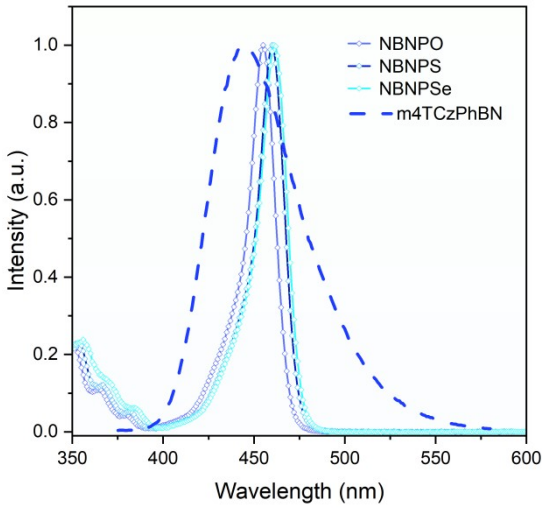

Fig. S33 UV-vis absorption spectra of NBNPO/S/Se and emission spectrum of m4TCzPhBN.

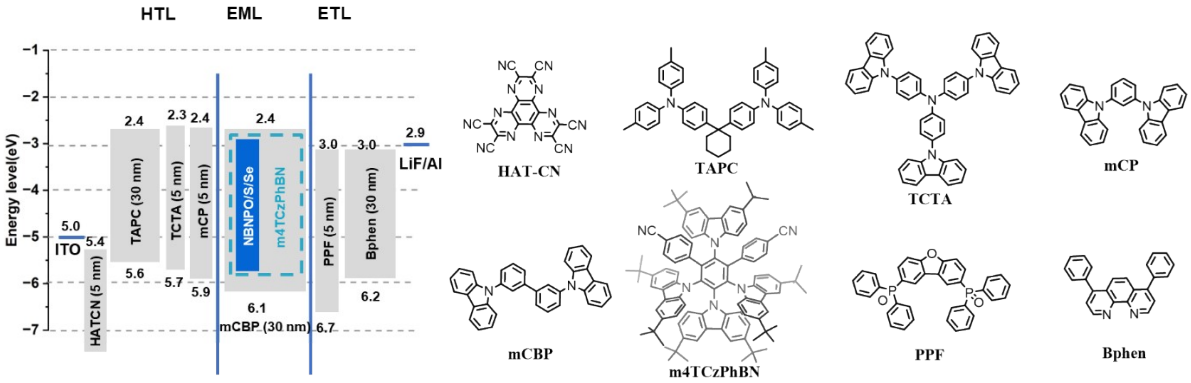

Fig. S34 Optimized OLED architecture based on NBNPO, NBNPS and NBNPSe materials and molecular structures of materials used in this study.

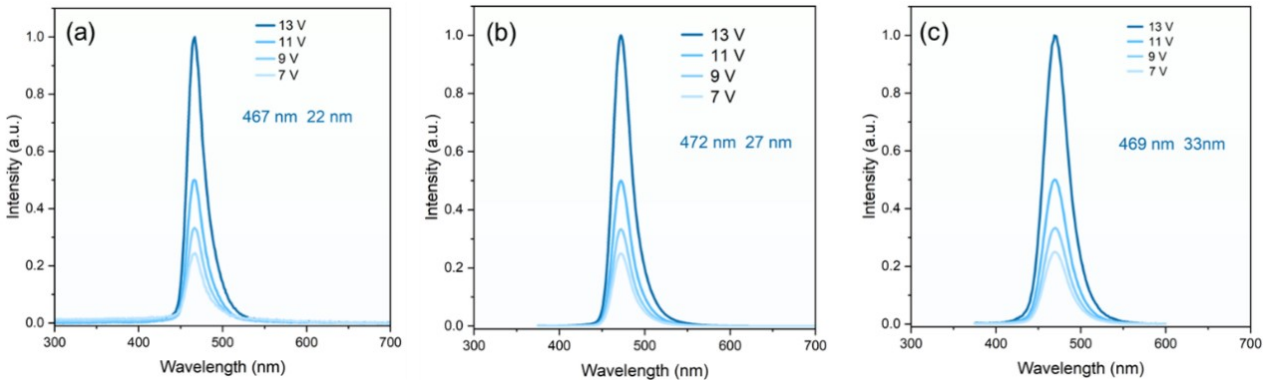

Fig. S35 Normalized EL spectra at different voltage of (a) D-NBNPO, (b) D-NBNPS, and (c) D-NBNPSe.

Table S15. Atomic locking strategy for efficient MR-TADF emitters based on DtCzB core.

Molecular structure	λ_{PL} (nm)	FWHM[a] (nm)	λ_{EL} (nm)	FWHM[b] (nm)	EQE_{max} (%)	Ref.
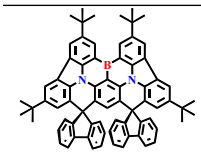	531	21	529	30	29.7	*Nat. Commun.* **2022**, *13*, 4876
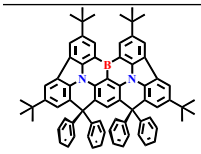	523	21	537	33	31.3	*Nat. Commun.* **2022**, *13*, 4876
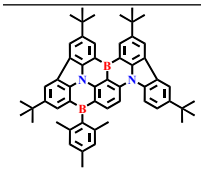	452	14	452	17	33.9	*Sci. Adv.* **2023**, *9*, eadh1434
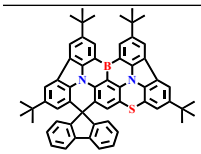	621	55	624	58	37.5	*Angew. Chem. Int. Ed.* **2024**, *9*, e202420253
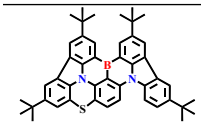	594	54	600	58	39.9	*Nat. Commun.* **2025**, *16*, 332
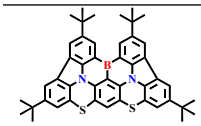	671	54	676	62	29.3	*Nat. Commun.* **2025**, *16*, 332

Reference

[1] M. J. Frisch, G. W. Trucks, H. B. Schlegel, G. E. Scuseria, M. A. Robb, J. R. Cheeseman, G. Scalmani, V. Barone, G. A. Petersson, H. Nakatsuji, X. Li, M. Caricato, A. V. Marenich, J. Bloino, B. G. Janesko, R. Gomperts, B. Mennucci, H. P. Hratchian, J. V. Ortiz, A. F. Izmaylov, J. L. Sonnenberg, D. Williams-Young, F. Ding, F. Lipparini, F. Egidi, J. Goings, B. Peng, A. Petrone, T. Henderson, D. Ranasinghe, V. G. Zakrzewski, J. Gao, N. Rega, G. Zheng, W. Liang, M. Hada, M. Ehara, K. Toyota, R. Fukuda, J. Hasegawa, M. Ishida, T. Nakajima, Y. Honda, O. Kitao, H. Nakai, T. Vreven, K. Throssell, J. A. Montgomery, Jr., J. E. Peralta, F. Ogliaro, M. J. Bearpark, J. J. Heyd, E. N. Brothers, K. N. Kudin, V. N. Staroverov, T. A. Keith, R. Kobayashi, J. Normand, K. Raghavachari, A. P. Rendell, J. C. Burant, S. S. Iyengar, J. Tomasi,

M. Cossi, J. M. Millam, M. Klene, C. Adamo, R. Cammi, J. W. Ochterski, R. L. Martin, K. Morokuma, O. Farkas, J. B. Foresman and D. J. Fox, Gaussian, Inc., Wallingford CT, 2016.

[2] T. Lu and F. W. Chen, *J. Comput. Chem*., 2012, **33**, 580.

[3] C. Li, Y. Luo, Y. Huang, H. Qiu and Z. Lu, *Anal. Chem.,* 2023, **95**, 8150.